

Kent Academic Repository

Full text document (pdf)

Citation for published version

Karatzafiri, Christina and Adamek, Nancy and Geeves, Michael A. (2017) Modulators of actin-myosin dissociation: basis for muscle type functional differences during fatigue. *American Journal of Physiology - Cell Physiology*, 313 (6). C644-C654. ISSN 0363-6143.

DOI

<https://doi.org/10.1152/ajpcell.00023.2017>

Link to record in KAR

<http://kar.kent.ac.uk/64123/>

Document Version

Author's Accepted Manuscript

Copyright & reuse

Content in the Kent Academic Repository is made available for research purposes. Unless otherwise stated all content is protected by copyright and in the absence of an open licence (eg Creative Commons), permissions for further reuse of content should be sought from the publisher, author or other copyright holder.

Versions of research

The version in the Kent Academic Repository may differ from the final published version.

Users are advised to check <http://kar.kent.ac.uk> for the status of the paper. **Users should always cite the published version of record.**

Enquiries

For any further enquiries regarding the licence status of this document, please contact:

researchsupport@kent.ac.uk

If you believe this document infringes copyright then please contact the KAR admin team with the take-down information provided at <http://kar.kent.ac.uk/contact.html>

1 Modulators of actin-myosin dissociation: basis for muscle type
2 functional differences during fatigue

3 100 characters incl. spaces

4 Authors: Christina Karatzaferi ^{1,2}, Nancy Adamek ³, and Michael A. Geeves ³

5 ¹ Muscle Physiology and Mechanics Group, DPESS, University of Thessaly, Karyes,
6 Trikala, 42100, Greece

7 ² Experimental Myology and Integrative Physiology Cluster, FSHS, University of St
8 Mark and St John, UK

9 ³ School of Biosciences, University of Kent, Canterbury, CT2 7NH Kent, UK

10

11 Running head: Muscle type actomyosin dissociation differences in fatigue

12 58 characters incl. spaces

13 Address for correspondence: M.A. Geeves, School of Biological Sciences, University
14 of Kent, Canterbury, CT2 7NH Kent, UK, M.A.Geeves@kent.ac.uk

15 Author contributions: CK & MAG conceived the study, MAG & CK designed the study,
16 NA & CK collected data, NA created figures and tables, all co-wrote and edited the
17 original manuscript, CK and MAG revised the manuscript.

18

19 **Abstract**

20 The muscle types present with variable fatigue tolerance, in part due to the myosin
21 isoform expressed. However, the critical steps that define 'fatigability' *in vivo* of fast
22 vs slow myosin isoforms, at the molecular level, are not yet fully understood. We
23 examined the modulation of the ATP-induced myosin sub-fragment 1 (S1)
24 dissociation from pyrene-actin by inorganic phosphate (Pi), pH and temperature
25 using a specially modified stopped-flow system that allowed fast kinetics
26 measurements at physiological temperature. We contrasted the properties of rabbit
27 psoas (fast) and bovine masseter (slow) myosins (obtained from samples collected
28 from New Zealand rabbits and from a licensed abattoir, respectively, according to
29 institutional and national ethics permits). To identify ATP cycling biochemical
30 intermediates, we assessed ATP binding to a pre-equilibrated mixture of actomyosin
31 and variable [ADP], pH (pH 7 vs pH 6.2) and Pi (zero, 15 or 30 added mM Pi) in a
32 range of temperatures (5 to 45°C). Temperature and pH variations had little, if any,
33 effect on the ADP dissociation constant (K_{ADP}) for fast S1 but for slow S1 K_{ADP} was
34 weakened with increasing temperature or low pH. In the absence of ADP, the
35 dissociation constant for phosphate (K_{Pi}) was weakened with increasing temperature
36 for fast S1. In the presence of ADP, myosin type differences were revealed at the
37 apparent phosphate affinity, depending on pH and temperature. Overall, the newly
38 revealed kinetic differences between myosin types could help explain the *in vivo*
39 observed muscle type functional differences at rest and during fatigue.

40 246 words

41

42 **Keywords:** myosin kinetics, cross-bridge cycle, temperature, muscle fatigue

43

44 **Introduction**

45 Myosin II exists in multiple isoforms (49) with *slow* muscles expressing the type 1
46 (MyHC-1 also known as β myosin) and *fast* muscles expressing one or more of the
47 type 2 myosins (MyHC-2a, 2b, or 2x). Contraction depends directly on the
48 interaction of myosin II multi-headed filaments, with filamentous 'tracks' of actin,
49 arranged within the sarcomeres, the 'functional units' of muscle (28, 47). Eventually,
50 whole muscle force output depends on the number of myosin cross-bridges
51 interacting 'strongly' or 'weakly' with actin, while the velocity of contraction
52 depends on the rate at which myosin detaches from actin at the end of the working
53 stroke (11).

54 The study of kinetics of the actomyosin (A.M) interaction cycle identifies clear
55 intermediate steps (for a review see (5)). Such studies have revealed that slow
56 skeletal myosin heavy chain isoforms (MyHC 1) have distinct properties from fast
57 isoforms (MyHC 2s), e.g. regarding ATPase activity and the rate and equilibrium
58 constants of the various biochemical steps, which are expected to dictate their
59 different mechanical properties. Thus, efficiency of actin-induced ADP displacement
60 from myosin (the ratio of the ADP dissociation constant for A.M (K_{ADP}) over the ADP
61 dissociation constant for myosin (K_D)), and strain sensitivity (dependence on external
62 mechanical load) can differ substantially between fast and slow myosins (5, 22) ,
63 with slow myosins binding ADP tightly and releasing it at a slower rate than fast
64 myosins. Consequently, ADP release is considered the rate limiting step for the
65 maximum contraction velocity of slow muscles (29, 44), at least at the temperatures
66 where fibers or myosin solutions are usually studied (10 to 22 °C).

67 The coupling of biochemical steps with mechanical events has, however, not been
68 fully elucidated (22) while the 'laws' governing how ensembles of myosins integrate
69 within the organized sarcomere (18, 19, 40) are not yet fully defined; this can be
70 attributed partly to lack of physiologically relevant experimental evidence at the
71 molecular level. This is especially true on the question of muscle fatigue, a complex
72 multifaceted phenomenon.

73 At the organismal level, fatigue has a large heterogeneity of research outcomes (6)
74 depending on the type, duration and intensity of muscular activity employed (8, 10),
75 the muscle composition studied (24) and health status (30), etc. In terms of
76 intramuscular biochemical changes, the degree of acidosis observed depends on the
77 rate and extent to which anaerobic glycolysis is relied upon; which in turn is
78 dependent on the fiber type and type of activity (i.e. more in 'supramaximal'/sprint
79 type work, more in ischemia) as well as the presence and activity of lactate and
80 proton transporters (see e.g. (32)). Brief very intense voluntary exercise has been
81 shown, in mixed muscle, to lower pH from 7.1 to 6.4 (7, 8, 27, 31, 48) and to disturb
82 the ATP and phosphocreatine levels, notably in fast, type II, fibers to near depletion
83 (34, 35). Based on NMR data, ADP levels are calculated to rise to 200 μM (21) as, in
84 healthy muscle, they are well buffered by the adenylate kinase and AMP deaminase
85 reactions (26). Still, small variations in [ADP] can significantly affect the sarcoplasmic
86 reticulum's function (39), and may help in maintaining tension economy (37). The
87 drop in pH affects not only calcium sensitivity (20) but also the effect of accumulated
88 P_i , which can reach 20-30mM in exercising muscle (2, 38), with its di-protonated
89 form considered to inhibit force (for a review see (2)). At the myofibrillar level,
90 changes in muscle mechanics during fatigue could be related to either reduction of
91 energy substrates (e.g. causing localized ATP minima (34, 35)) and /or accumulation
92 of ATP hydrolysis by-products (e.g. (14, 33, 37, 45, 53)). This is because the
93 interaction of myosin with actin (actomyosin) is a multi-substrate and multistep
94 reaction i.e. not only fueled by ATP hydrolysis but also modulated by ATP hydrolysis
95 by-products (ADP, P_i , H^+) and other prevailing intracellular conditions (12). Thus, for
96 the purposes of this work, fatigue is considered in the context of factors influencing
97 the actomyosin cycle in a way to cause slowing of the cycle and/or weaker
98 actomyosin interactions.

99 Overall, investigations ranging from whole body exercise (8, 30), to intact small
100 muscles or fibers (59) to skinned fibers, (13, 14, 17, 33, 37, 46) or myofibrils (53),
101 and few isolated molecule approaches [e.g. (16)] have provided strong evidence that
102 the accumulation of inorganic phosphate (P_i) and of hydrogen ions can contribute to,
103 if not cause, peripheral muscle fatigue. Still, their exact impact, especially at

104 physiological *in vivo* conditions, has attracted much debate (e.g. (58)). This is further
105 complicated by muscle type differences (fast vs slow) in energetics, myosin ATPase,
106 and mechanical performance (9, 49, 50) , which can be linked to a great degree to
107 inherent properties of the myosin II isoform expressed.

108 Our understanding of fatigue effects is further complicated by muscle type
109 differences (fast vs slow) in energetics, myosin ATPase, and mechanical performance
110 (9, 49, 50) , which can be linked to a great degree to inherent properties of the
111 myosin II isoform expressed. The steps that control the detachment of the myosin
112 cross-bridge at the end of the working stroke from actin are rapid and are thought to
113 limit the shortening velocity, a key parameter of muscle function. Temperature
114 predictions from kinetic studies of actomyosin in solution (44), suggest that the rate
115 of ADP release may limit unloaded velocity for both fast and slow myosin isoforms. It
116 can be hypothesized that such an ADP effect could be aggravated by the presence of
117 hydrogen ions and inorganic phosphate, as in fatigue, but it is not known if this is the
118 case and what would be the role of the myosin type.

119 Moreover, a parameter not often considered is temperature. *In vivo* mammalian
120 muscle temperature ranges from 32 to > 40 °C, while in severe fatigue, pH drops and
121 inorganic phosphate (Pi) accumulates (23) concomitantly. A number of *in vitro* fiber
122 studies at higher temperatures, have challenged long held views about the individual
123 role of the key 'fatigue' metabolites on mechanics, [e.g. less of an effect of pH (36,
124 45, 59)) or Pi on force, (13, 14, 17, 33)]. Thus, it appears that employing
125 temperature modulations in the *in vitro* experimentation is necessary to tease out
126 physiological synergies [e.g. a synergism of myosin light chain phosphorylation with
127 low pH and high [Pi] became evident only at a high temperature (36)], if one wants
128 to realistically link muscle function *in vivo* to actomyosin interaction molecular
129 events studied *in vitro*. This necessitates molecular experimentation that mimics
130 physiology to the degree possible.

131 Therefore the purpose of this research was to study the fast kinetics of ATP-induced
132 dissociation of A.M. with and without ADP using the stopped flow. We examined the
133 interplay of 'fatigue' factors, e.g. low pH and high inorganic phosphate (Pi), with

134 myosin type, on ATP-induced dissociation of A.M. Taking advantage of recent
135 methodological advancements we studied, for the first time, the ATP-induced
136 dissociation of fast and slow S1 from actin in temperatures ranging from 5 to 45 °C to
137 reveal critical myosin type and/or temperature dependencies of these processes.

138

139 *Glossary & abbreviations*

140 A.M: actomyosin complex

141 S1: myosin subfragment 1

142 actin.S1: actin bound with S1

143 K_1 : equilibrium constant for the formation of the complex of AM with ATP (denoted
144 as A.M.T),

145 k_{+2} : rate constant of isomerization of A.M.T to A~M.T which is followed by actin
146 dissociation

147 k_{obs} : observed rate constant of ATP induced dissociation of myosin from actin

148 K_{ADP} : dissociation constant for ADP

149 K_{Pi} : dissociation constant for phosphate

150 K_{ADP+Pi} : dissociation constant for ADP in the presence of phosphate

151 MyHC: myosin heavy chain

152

153 ***Materials and methods***

154 **Ethics Statement**

155 Muscle tissue was obtained post-mortem from animals treated as recommended by
156 national and local guidelines (UK Animals (Scientific Procedures) Act, 1986). Fast
157 skeletal muscle came from the psoas muscle of New Zealand rabbits and slow
158 skeletal muscle from bovine masseter.

159 **Protein preparation**

160 Myosin was prepared from the rabbit psoas (for fast MyHC-II) and the bovine
161 masseter muscle (for slow MyHC-I) according to Margossian and Lowey (41) , and
162 was subsequently digested to subfragment 1 (S1) with chymotrypsin as described by
163 Weeds & Taylor (57) which removes the regulatory light chain region. These two
164 muscle types yield essentially pure MyHC isoform (e.g. (1, 25) for rabbit psoas
165 (isoform 2X) and (55) for bovine masseter (isoform 1) a result confirmed in routine

166 SDS-PAGE by us and others and by the expected value of K_{ADP} which is characteristic
167 of a pure MyHC isoform (as indicated e.g. in (4)).

168 Actin was prepared from rabbit muscle as described by Spudich & Watt (52) and
169 labelled with pyrene iodoacetamide to give pyrene-labelled actin as described by
170 Criddle et al (15). Protein stocks of S1 and of pyrene-labelled actin were stored at 4°C
171 and were used for up to 2 weeks. In the text herein reference to actin implies
172 pyrene-labelled actin.

173

174 **Experimental buffers**

175 The main buffer contained 20 mM cacodylate (adjusted at pH 7.0 or pH 6.2), 100
176 mM KCl, 5 mM MgCl₂ and 1 mM NaN₃; when phosphate was present in the buffer
177 the ionic strength was adjusted accordingly to a final ionic strength of 170 mM.
178 Concentrations (whether of proteins or buffer constituents) given in the text and
179 figure legends refer to the concentration after mixing 1:1 in the stopped flow (unless
180 stated otherwise).

181

182 **Experimental equipment, procedures and analysis**

183 Stopped-flow experiments were performed essentially as described previously (4)
184 using a HiTech Scientific SF-61DX2 stopped flow system and 4-5 transients were
185 acquired for each ATP transients (Kinetic Studio suite). The dead time of the
186 equipment was 0.002 s. A wide temperature range (5 – 45 °C) for measurements
187 was available because of a new adaptation of the standard stopped flow machine
188 (see (56)). Briefly, the drive syringes were held at room temperature (20 °C) while
189 loading lines leading into the mixing chamber, the mixing and observation chamber
190 were all thermostated at the temperature of the measurement. Essentially the
191 samples were only exposed to the temperature of the measurement for a few
192 seconds, thus allowing measurements of proteins under conditions where they are
193 not usually stable for long.

194

195 The **ATP induced dissociation rate of actin.S1**, was measured in the stopped-flow by
196 mixing a fixed concentration of pyr.actin.S1 complex (end concentration 0.25 μM)
197 with excess ATP and monitoring fluorescence transients from the pyrene-labeled

198 actin (excitation at 365 nm, emission through a KV389 nm cut-off filter (Schott,
199 Mainz, Germany)). Details of the kinetic analysis are given under data fitting.

200

201 In a similar process, **ADP dissociation constant** (K_{ADP}), which defines ADP affinity for
202 actin.S1, was measured by adding to the mixture ADP as a competitive inhibitor of
203 ATP binding. In this case it is convenient to add the ADP to the ATP solution, i.e. 0.5
204 μM pyr.actin.S1 was mixed with 25 μM ATP with various concentrations of ADP
205 present with the ATP (from 0 to 1200 μM). This approach assumes that ADP is in
206 rapid equilibrium with the actin.S1 complex on the time scale of the ATP induced
207 dissociation reaction. This was ensured by using the low (25 μM) concentration of
208 ATP. That this assumption holds was tested by repeating the measurement with
209 ADP pre-incubated with actin.S1 and then mixing with ATP. The observed rate
210 constants were identical in each case. Details of the data analysis are given below
211 (see Scheme 1 on the competitive inhibitor approach, and equation 4).

212

213 **Phosphate dissociation constant** (K_{Pi}) was measured exactly as for the ADP
214 dissociation constant except that the high concentrations of P_i used meant it was
215 more convenient to have P_i present in the buffer in both syringes of the stopped-
216 flow. Details of the data analysis are given below (see Scheme 1 on the competitive
217 inhibitor approach, and equations 5 and 6).

218

219 **ADP dissociation constant in the presence of phosphate** (K_{ADP+Pi}) was also measured
220 using the same approach as for K_{ADP} but using buffers containing fixed amounts of
221 inorganic phosphate, 30 mM in the case of psoas S1 and 15 mM with masseter S1.
222 The different affinities of P_i for the two types of S1 required a different
223 concentration of P_i . Preliminary data indicated that P_i binding to psoas S1 was > 10
224 mM and weaker than to masseter S1, by approximately a factor of 2. Since the limits
225 of ionic strength precluded using saturation amounts of P_i we used a P_i
226 concentration close to the range of K_{Pi} values.

227

228 Experiments were performed at two pH levels, 7 and 6.2 and in a range of
229 temperatures. Care was taken to reverse the order of experiments to avoid the

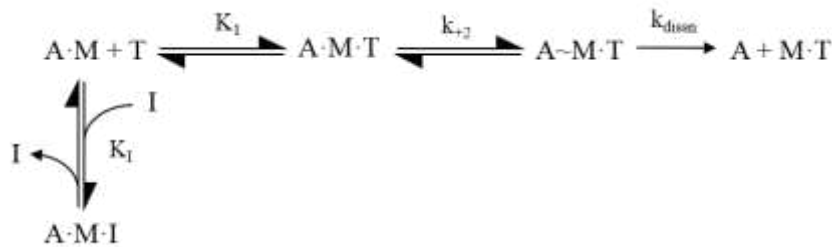
230 possibility of a time and 'order' effect either with respects to pH or temperature.

231

232 **Data Fitting and Interpretation Approach**

233 In the present study we focused our attention on the ATP induced dissociation of
234 actin.S1. This is the step that controls the detachment of the actomyosin cross-
235 bridge at the end of the working stroke.

236



237

238 **Scheme 1.** Model of ATP-induced dissociation of actin.S1 based on Millar and Geeves
239 (42) .

240

241 In Scheme 1, T = ATP; A = actin; M = myosin; I is an inhibitor, competitive with ATP
242 for the nucleotide binding site. K_1 defines the equilibrium constant for the formation
243 of the A.M.T collision complex, which is followed by an almost irreversible
244 isomerization of the complex to the ternary complex A~M.T with the rate constant of
245 k_{+2} . This is rapidly followed by dissociation of actin from the ternary complex. K_i is
246 defined as a dissociation constant k_{-i}/k_{+i} . In the experiments presented here the
247 inhibitor was either ADP or inorganic phosphate (P_i).

248

249 The reaction described in Scheme 1 was monitored through pyrene fluorescence
250 changes which monitor the ATP induced dissociation of actin from the complex
251 (fluorescence increases by up to 70 %.), specifically associated with step 2 of Scheme
252 1, (see in Results, Fig. 1A). Four to five transients were collected for each ATP
253 concentration used then averaged before further analysis.

254

255 The averaged transients were fitted with single (eqn1) or, if needed, a double
256 exponential equation (eqn2):

257

$$258 \quad F_t = \Delta F \cdot e^{(-k_{obs} \cdot t)} + F_\infty \quad eqn 1$$

259 or

$$260 \quad F_t = \Delta F_{(1)} \cdot e^{(-k_{obs(1)} \cdot t)} + \Delta F_{(2)} \cdot e^{(-k_{obs(2)} \cdot t)} + F_\infty \quad eqn 2$$

261

262 Where F_t is the observed fluorescence at time t , F_∞ is the fluorescence at the end of
263 the transient ($t = \infty$) and ΔF is the total change of fluorescence observed. The
264 observed rate constant (k_{obs}) reflects the ATP induced dissociation rate of actin.S1
265 and is linearly dependent on $[ATP]$, at the ATP concentrations used here. A plot of
266 $[ATP]$ vs k_{obs} was used to derive the values of K_1 and k_{+2} (using Origin v 6.0), as
267 defined in scheme 1 and eqn 3.

268

269

$$k_{obs} = K_1 k_{+2} [ATP] \quad eqn\ 3$$

270

271

272 The presence of a competitive inhibitor to ATP binding (that does not induce actin.S1
273 dissociation) would appear to slow the rate of actin.S1 dissociation. If inhibitor
274 binding is in rapid equilibrium with actin.S1, within the timescale of data acquisition,
275 compared to the rate of ATP-induced dissociation of actin.S1 (i.e. $k_{+AD} + [ADP]k_{-AD} \gg$
276 $K_1 k_{+2} [ATP]$), then

277

278

$$k_{obs} = K_1 k_{+2} [ATP] / (1 + ([I]/K_i)) \quad eqn\ 4$$

279

280 Then, plotting k_{obs} as a function of $[I]$ will allow the K_i (in scheme 1) to be defined.
281 This approach was used to define the value of K_i for ADP (K_{ADP}) and Pi (K_{Pi}).

282

283 If both ADP and Pi are present in the same measurement, two scenarios are possible.
284 If both compete for the same binding site then the effect of the two inhibitors is
285 additive and the effect on k_{obs} can be predicted from the values of K_{ADP} and K_{Pi}
286 measured independently.

287

288

$$k_{obs} = K_1 k_{+2} [ATP] / (1 + ([ADP]/K_{ADP}) + ([Pi]/K_{Pi})) \quad eqn\ 5$$

289

290 where the measured K_i with variation of $[ADP]$ and fixed $[Pi]$ is $K_i = 1/K_{ADP} +$
291 $[Pi]/K_{Pi}$

292

293 If both however bind into the ATP pocket at the same time to create the complex
294 A.M.ADP.Pi then the above relationship will not hold and Pi will alter the affinity of
295 A.M for ADP.

296

297 The apparent affinity of ADP for actin.S1 (K_{ADP+Pi}) was measured for several
298 concentrations of Pi and then the dissociation constant of Pi calculated according to
299 the following relationship and compared with the value of K_{Pi} .

$$300 \quad K_{Pi \text{ app}} = [Pi]/(K_{ADP+Pi}/K_{ADP} - 1) \quad \text{eqn 6}$$

301
302

303 *ADP release rate constant.* Two types of myosins were studied which are known to
304 differ in their dissociation constant for nucleotides (5, 51). The rate constant for the
305 release of ADP (k_{ADP}) is relatively slow for masseter S1 and can easily be measured in
306 an ADP displacement experiment. This step is very fast for a fast muscle isoform and
307 too fast to measure by current equipment. Briefly, actin.^{Mass}S1 saturated with 75
308 μ M of ADP (A.M.D complex) was mixed with a large excess of ATP (8 mM) in the
309 stopped-flow. Then the k_{obs} values, fitted to a single exponential equation (eqn 1)
310 defined the rate constant by which ADP is released by the ternary A.M.D complex (k_{AD}).
311

312

313 The data presented in the figures are the values for the individual experiment
314 displayed, while the data values presented in the table 1 are averaged values for n =
315 independent day measurements.

316

317 The *temperature dependence* of the above studied biochemical steps K_{1k+2} , K_{ADP} , K_{Pi}
318 and K_{ADP+Pi} data were plotted as the natural logarithm of the measured parameter
319 against the reciprocal of temperature in degrees Kelvin ($1/T$ °K) and fitted with linear
320 regression using the Arrhenius (rate constants) or Van't Hoff (equilibrium constants)
321 equations

322

$$323 \quad \ln K_{1k+2} = \ln(A) - E_a/RT \quad \text{eqn 7}$$

324

$$325 \quad \ln K_{eq} = \Delta S^\circ/R - \Delta H^\circ/RT \quad \text{eqn 8}$$

326

327 where E_a stands for activation energy, R is the gas constant, A is a pre-exponential
328 factor. The values of $-E_a/R$ or $\Delta H^\circ/R$ were derived from the slopes.

329

330 **Results & Discussion**

331 **ATP induced dissociation rate of actin.S1.** When actin.^{Pso}S1 and actin.^{Mass}S1 were
332 mixed with ATP, as shown in Figure 1 A and B, the observed stopped-flow transients
333 were described by a single exponential for both myosin isoforms (Fig 1A and 1B).
334 Keeping a fixed ATP concentration and increasing the temperature allows the best
335 estimate of the temperature dependence of the reaction since it minimizes variation
336 in ATP concentration between experiments. Increasing the temperature from 5-43
337 °C reduced the total fluorescence signal by ~ 40% due to collisional quenching but
338 the signal change remained relatively constant with an approximately 2-fold increase
339 in fluorescence observed in all transients. The transients were therefore normalized
340 to illustrate the change in the k_{obs} values. For *psoas* (Fig 1 A) and *masseter* (Fig 1 B)
341 temperature increased the k_{obs} value ~3 fold in both cases over the range of
342 measurements from 3 to 43 °C. The figure shows illustrative examples of one set of
343 transients.

344 Lowering the pH to 6.2 slightly increased the k_{obs} values for both isoforms by about
345 20-25 % (and hence the second order rate constant K_1k_{+2} , see Table 1). Increasing
346 temperature resulted in an average increase of 3 fold over the temperature range of
347 5-35 °C. The amplitudes of the transients at pH 6.2 were again relatively stable and
348 similar to pH 7 for ^{Pso}S1 at 43 %. For ^{Mass}S1 the amplitudes were also stable in pH 6.2
349 but showed an overall increase in fluorescence from 40 to 50% of total fluorescence
350 signal.

351 *Effect of temperature:* The temperature dependence of the dissociation rate
352 constant was examined at pH 7 and then repeated at pH 6.2 (Fig 1C and 1D). Each
353 measurement was repeated 3 times and the average values collated in Table 2. The
354 Arrhenius plots of the temperature dependence measurements at pH 7 and 6.2 gave
355 well defined straight lines over the temperature range (5 – 43 °C). In the absence of
356 phosphate, for *psoas* the activation energy (E_a) values were very similar at pH 7.0
357 and 6.2 as shown in Figure 1 C, 28.3 ± 0.8 and 29.3 ± 0.8 kJ/mol respectively. For
358 *masseter*, E_a values were on average lower than the ones for fast, being for pH 7.0
359 and 6.2, 25.7 ± 1.4 and 23.8 ± 1.1 kJ/mol respectively (Figure 1D).

360 *Effect of Pi and pH:* When the ATP-induced dissociation measurements were
361 repeated in the presence of high phosphate concentrations, of the order that might
362 be expected in fatigue, the observed rate constants for the dissociation reaction
363 were 2-fold slower for ^{Mass}S1 and 2- to 3-fold slower for ^{Pso}S1 at both pH levels
364 compared to the data in the absence of phosphate. This is consistent with Pi acting
365 as a competitive inhibitor with a K_i of 10 – 20 mM. It should be noted that while 30
366 mM Pi was used for ^{Pso}S1, 15 mM Pi was used for ^{Mass}S1 experiments.

367 The transients of both isoforms had bi-phasic tendencies at the low temperatures (5-
368 10 °C) at both pHs, but were single exponential at all other temperatures. The origin
369 of this additional slow phase, which had a very small amplitude (1-3 %), is not
370 known, but possible contamination by ADP was eliminated by control measurements
371 in the presence of apyrase which converts any ADP present, which does not bind to
372 S1, to AMP.

373 The amplitudes of the dissociation reaction were 50 % smaller/reduced in the
374 presence of phosphate for both, ^{Pso}S1 and ^{Mass}S1, indicating some loss of affinity of
375 S1 for actin in the presence of Pi. However, for *psoas* the amplitudes increased with
376 temperature from 25 to 30 % at pH 7.0 and even more dramatically from 12 to 20 %
377 at pH 6.2. This behavior was not observed with ^{Mass}S1 *masseter*.

378 *Combined effect of temperature, pH and phosphate:* the temperature dependence of
379 the dissociation rate constant in the presence of phosphate is shown in Figure 2 and
380 the activation energies determined for *psoas* (38 ± 1 kJ/mol) and *masseter* (30 ± 1
381 kJ/mol) were greater than in the absence of Pi, irrespective of the pH used. Thus
382 phosphate increased the activation energy of ^{Pso}S1 at both pH values by about 10
383 kJ/mol, which is a larger increase than observed with *masseter*, where the increase
384 was only about 5 kJ/mol in the presence of phosphate.

385 **Rate constant of ADP release (k_{ADP})** was evaluated by an ADP displacement
386 experiment, mixing actin.^{Mass}S1 saturated with ADP with an excess of ATP. This
387 measurement was not possible for ^{Psoas}S1 because the ADP release is too fast to
388 measure.

389 Displacement of ADP from actin.^{Mass}S1 by a large excess of ATP was biphasic. The
390 transients were well-defined with stable amplitudes of 24 and 6 % for the fast and
391 slow phase, respectively (as shown in Figure 3 A). These amplitudes were similar
392 under all conditions explored. The fast phase defines the rate constant at which ADP
393 is released and is thought to limit the velocity of shortening of a masseter muscle (4).
394 The slower phase is an off pathway event and will not be considered further here.
395 The k_{obs} of the ADP release was 85 s^{-1} at $20 \text{ }^\circ\text{C}$ (pH 7.0) and compares well to
396 published results of 94 s^{-1} by Bloemink et al (4).

397

398 The reaction was measured over the temperature range of $5 - 30 \text{ }^\circ\text{C}$ at pH 6.2 and
399 7.0, and in the presence of 15 mM Pi. The k_{obs} values are summarized in the
400 Arrhenius plot in Fig 3B. The k_{obs} values increased from 16.2 at $5 \text{ }^\circ\text{C}$ to 273 s^{-1} at $30 \text{ }^\circ\text{C}$
401 with similar values at pH 7.0 and pH 6.2 throughout the temperature range used.
402 Above $30 \text{ }^\circ\text{C}$ the reaction was too fast to measure reliably. Thus the activation
403 energy was large with similar values at both pH levels studied.

404 The addition of 15 mM Pi had little effect at pH 7.0. At pH 6.2 however we saw a 30-
405 50 % increase in k_{obs} in the presence of phosphate and a small change in the
406 activation energy.

407

408 **ADP dissociation constant (K_{ADP})**

409 The ADP dissociation constant (K_{ADP}) for pyr.actin.S1 was measured by the
410 competitive inhibitor approach as described in the Methods.

411 ADP included in the ATP solution competes with ATP for binding to the pyr.actin.S1
412 and slows the k_{obs} value as shown in Fig 4. The ADP dissociation constant was 168
413 μM for ^{Pso}S1 and $31 \mu\text{M}$ for ^{Mass}S1 at $20 \text{ }^\circ\text{C}$ and pH 7.0, as reported previously (22).
414 This large difference in the affinity of actin.S1 for ADP is a major characteristic of a
415 fast vs a slow myosin isoform. As reported previously the ADP affinity for *psaos*
416 actin.S1 was relatively unaffected by temperature (about $200 \pm 30 \mu\text{M}$ between 10

417 and 30 °C) while for *masseter* the effect was much greater, with the affinity
418 becoming weaker by ~6-fold from 9.6 μM at 10 °C to 62.4 at 30 °C, at pH 7.0.

419 *Effect of pH:* A change in pH did not affect the ADP affinity for *psaos* (Table 1) over
420 the temperature range studied (also Figure 4C). Lowering the pH to 6.2 with $^{Mass}S1$
421 resulted in 2-fold weaker K_{ADP} values than at pH 7.0 (from 10 to 22 μM at 10 °C).
422 However, this effect of pH was not as pronounced at higher temperatures (only
423 weakening by 1.5 fold at 30 °C, see Table 1).

424

425 **Phosphate dissociation constant (K_{Pi})**

426 The dissociation constant of Pi for actin.S1 (K_{Pi}) was measured but the range of Pi
427 concentrations accessible was restricted by the need to maintain a constant ionic
428 strength. As Pi was increased the concentration of KCl in the buffer was decreased
429 and the maximum phosphate concentration used was 30 mM. Figure 6 shows the
430 plots of k_{obs} as a function of phosphate concentration for the two myosin isoforms.
431 These show the expected inhibition as [Pi] is increased with an average K_{Pi} value of
432 15 mM at 10 °C decreasing to 41 mM at 40 °C for actin. $^{Pso}S1$ at pH 7.0. Decreasing
433 the pH to 6.2 did not significantly affect the K_{Pi} values for $^{Pso}S1$ (11 mM at 10 °C,
434 decreasing to 32 mM at 40 °C, see also Table 1).

435 Repeating the measurements with $^{Mass}S1$ gave a K_{Pi} of 22 mM at 10 °C, weakened to
436 35 mM at 20 °C (pH 7.0). Lowering the pH to 6.2 resulted in an average K_{Pi} value of
437 17 mM at 10 °C, weakening to 28 mM at 40 °C. Thus a differential response of slow
438 myosin to Pi was observed with temperature, with the slow myosin while starting off
439 less sensitive to Pi at 10°C becoming more sensitive to Pi at 40°C.

440

441 **ADP dissociation constant in the presence of phosphate (K_{ADP+Pi})** was evaluated as
442 for the ADP dissociation constant but using fixed amounts of inorganic phosphate
443 (30 mM in the case of $^{Pso}S1$ and 15 mM with $^{Mass}S1$). The presence of 30 mM Pi
444 weakened the ADP dissociation constant (K_{ADP+Pi}) for actin. $^{Pso}S1$ 3-4-fold (from about
445 170 μM to 890 μM at 20 °C (pH 7.0)) as shown in Figure 5A and Table 1. Repeating

446 the measurement at different temperatures showed the apparent K_{ADP} weakening
447 from around 500 μM at 10-20 $^{\circ}\text{C}$ to 942 μM at 30 $^{\circ}\text{C}$ (Fig 5C and Table 1). For
448 *masseter* the effects of Pi were less marked, with the K_{ADP} weakening only 1-2-fold
449 across the temperature range at pH 7.0. Overall, it appears that phosphate competes
450 with ADP binding to fast A.M, but has little effect on ADP binding in slow A.M. The
451 formation of an A.M.ADP.Pi complex (see *Data Fitting and Interpretation Approach*)
452 is not supported under our experimental conditions.

453 Lowering the pH to 6.2 resulted in a smaller effect of phosphate on the ADP
454 dissociation constant for actin. $^{P50}S1$, changing only 2-fold from 228 to 514 μM at 20
455 $^{\circ}\text{C}$ (compared to the 3 to 4-fold change seen at pH 7.0). This reduced effect of
456 phosphate was seen across the temperature range used. In actin. $^{Mass}S1$, 15 mM Pi
457 weakened the ADP affinity 2-fold from 47 to 94 μM at 20 $^{\circ}\text{C}$, and a similar 2-fold
458 weakening of the K_{ADP} in phosphate (K_{ADP+Pi}) was seen at the other temperatures
459 used at pH 6.2.

460 **Apparent phosphate dissociation constant ($K_{Pi\ app}$)**

461 The apparent dissociation constant of phosphate for acto-myosinS1 ($K_{Pi\ app}$) in the
462 presence of ADP was calculated from the ADP dissociation constants measured in
463 the absence (K_{ADP}) and presence of phosphate (K_{ADP+Pi}) as detailed in the methods. At
464 pH 7.0 and low temperature the $K_{Pi\ app}$ of actin. $^{P50}S1$ was similar to the K_{Pi} value
465 measured (11mM and 16 mM, respectively at 10 $^{\circ}\text{C}$). At higher temperatures the K_{Pi}
466 of actin. $^{P50}S1$ was weakened to 30-40 mM, the $K_{Pi\ app}$ however remained at about 10
467 mM for the whole temperature range used.

468 At pH 6.2 the K_{Pi} of *psoas* was 30 % tighter than at pH 7.0 but otherwise showed the
469 same behavior as temperature was increased (weakening from 15 mM at 10 $^{\circ}\text{C}$ to 32
470 mM at 40 $^{\circ}\text{C}$). The $K_{Pi\ app}$ however appears 2-fold weaker at pH 6.2 for *psoas* with 24
471 mM and tightens to about 16 mM as temperature is increased.

472 For actin. $^{Mass}S1$ we observed a different behavior of the apparent phosphate
473 dissociation constant; while the measured K_{Pi} values at pH 7.0 were similar to *psoas*
474 across the temperature range used, the $K_{Pi\ app}$ showed distinct temperature
475 dependence, weakening from 10 to 40 mM with temperature. The K_{Pi} values of

476 *masseter* were unaffected by a change in pH to 6.2 and remained similar to *psoas* at
477 22 and 35 mM (10 and 20 °C, respectively). The $K_{Pi\ app}$ however lost its temperature
478 dependence when the pH was lowered to 6.2 and the value remained relatively
479 unaffected at 10-15 mM for actin.^{Mass}S1 throughout the temperature range used.

480 *Relevance to working muscle.* Work by us and others indicated an important role for
481 Pi in tension generation as conditions that affect actomyosin affinity, would affect, in
482 proportion, force generation. With the assumption that A.M force-generating states
483 are in an effective equilibrium with the non-force-generating states at the beginning
484 of the working stroke, past skinned *psoas* fiber work suggested that, with increasing
485 [Pi] the free energy of the states that precede Pi release decrease as $-RT \ln[Pi]$ (from
486 the slope of the force- $\ln[Pi]$ relationship, relative to the free energy of states after Pi
487 release, leading to progressive depopulation of the force-generating states and thus
488 reducing tension generation (33). Earlier observations by Tesi et al (54) highlighted
489 differences between slow and fast myofibrils in tension response to phosphate, with
490 indications of stronger actomyosin bonds in slow muscle. The combination of low pH
491 and high Pi was shown to synergistically inhibit velocity of contraction in skinned
492 fibres (36, 43) adding further support to the notion that in fatigue conditions, the
493 combined effect of Pi and protons on muscle performance would come about either
494 by decreasing the force per bridge and/or increasing the number of low-force
495 bridges. These and other studies indicated that the effect of Pi on its own is
496 moderate at higher temperatures but in combination with low pH it can substantially
497 affect muscle power by affecting actomyosin interaction. The present work adds
498 important information to explain how Pi's interaction changes the ADP dissociation
499 constant for AM and ultimately ATP-induced dissociation of AM, thus the speed of
500 the cross-bridge cycle.

501 *Concluding remarks*

502 The phenomena we studied are at a lower level of component configuration, actin
503 and myosin S1 in solution. We cannot therefore account for myosin cooperativity
504 and coordinated responses to load, which could affect the hypothesized limiting
505 processes. While experimental data imply such cooperativities (3) emerging

506 behaviors are difficult to assess and model, a situation further complicated by the
507 difficulty of incorporating intra-head actions into models (40). At the macroscopic
508 level, many studies have examined fatigue effects on mechanical function using
509 single fibers (most however at non-physiological temperature); there are also
510 isolated muscle and whole limb investigations (however with no control over
511 metabolites levels); all these macroscopic studies have theorized about what may be
512 occurring at the molecular level. Fewer studies have attempted a ‘molecular
513 explanation’ of how velocity is affected in muscle fatigue (e.g. using in vitro motility
514 (16)). Ours is the first study to employ solution transient kinetics to study how key
515 fatigue factors affect the ATP-induced dissociation step of fast and slow S1 from
516 actin (a critical part of the cycle that affects overall velocity). More information of
517 the other events in the cycle, and the temperature dependence of these events for
518 both fiber types, is needed to support future modelling attempts.

519 It remains to be seen how our findings can be integrated at the higher level
520 ‘behavior’ of large myosin ensembles interacting with actin filaments, outside or
521 inside an organized sarcomere. It is expected that in such situations other laws may
522 apply when the myosin type effect on contractile behavior is further modulated
523 depending on interactions with intracellular factors and overall muscle action
524 regulation.

525 We expect that, given the undisputed phenotypic effect of myosin types as observed
526 in mammalian physiology, our data provide highly relevant insights in the
527 mechanochemical coupling factors that distinguish the fiber types. Phosphate
528 dependence of ATP-induced dissociation is modulated by variations in actin affinity.
529 Such variations could help modulate the phosphate dependence of force and
530 velocity, and may explain why phosphate sensitivity appears to be in part
531 temperature-and muscle type-dependent.

532

533 **Acknowledgements**

534 The authors acknowledge support from various sources as follows:

535 MAG was supported by the British Heart Foundation grant PG30200. Also, CK, MAG
536 research was co-financed by the European Union (European Social Fund – ESF) and
537 Greek national funds through the Operational Program “Educational and Lifelong
538 Learning” of the National Strategic Reference Framework (NSRF) – Research Funding
539 Program: Thales (MuscleFun Project-MIS 377260) Investing in knowledge society
540 through the European Social Fund.

541 CK thanks COST Action CM1306 ‘Understanding Movement and Mechanism in
542 Molecular Machines’ for relevant networking support.

543

544

545

546

547 **References**

- 548 1. **Aigner S, Gohlsch B, Hamalainen N, Staron RS, Uber A, Wehrle U, and Pette D.** Fast
549 myosin heavy chain diversity in skeletal muscles of the rabbit: heavy chain IId, not IIb
550 predominates. *European journal of biochemistry* 211: 367-372, 1993.
- 551 2. **Allen DG, and Trajanovska S.** The multiple roles of phosphate in muscle fatigue.
552 *Frontiers in physiology* 3: 463, 2012.
- 553 3. **Baker JE.** Muscle force emerges from dynamic actin-myosin networks, not from
554 independent force generators. *American journal of physiology Cell physiology* 284: C1678;
555 author reply C1678-1679, 2003.
- 556 4. **Bloemink MJ, Adamek N, Reggiani C, and Geeves MA.** Kinetic analysis of the slow
557 skeletal myosin MHC-1 isoform from bovine masseter muscle. *Journal of molecular biology*
558 373: 1184-1197, 2007.
- 559 5. **Bloemink MJ, and Geeves MA.** Shaking the myosin family tree: biochemical kinetics
560 defines four types of myosin motor. *Seminars in cell & developmental biology* 22: 961-967,
561 2011.
- 562 6. **Bogdanis GC.** Effects of physical activity and inactivity on muscle fatigue. *Frontiers in*
563 *physiology* 3: 142, 2012.
- 564 7. **Bogdanis GC, Nevill ME, Boobis LH, Lakomy HK, and Nevill AM.** Recovery of power
565 output and muscle metabolites following 30 s of maximal sprint cycling in man. *The Journal*
566 *of physiology* 482 (Pt 2): 467-480, 1995.
- 567 8. **Bogdanis GC, Nevill ME, Lakomy HK, and Boobis LH.** Power output and muscle
568 metabolism during and following recovery from 10 and 20 s of maximal sprint exercise in
569 humans. *Acta physiologica Scandinavica* 163: 261-272, 1998.
- 570 9. **Bottinelli R.** Functional heterogeneity of mammalian single muscle fibres: do myosin
571 isoforms tell the whole story? *Pflugers Archiv : European journal of physiology* 443: 6-17,
572 2001.
- 573 10. **Cannon DT, Howe FA, Whipp BJ, Ward SA, McIntyre DJ, Ladroue C, Griffiths JR,**
574 **Kemp GJ, and Rossiter HB.** Muscle metabolism and activation heterogeneity by combined
575 ³¹P chemical shift and T2 imaging, and pulmonary O₂ uptake during incremental knee-
576 extensor exercise. *Journal of applied physiology* 115: 839-849, 2013.
- 577 11. **Cooke R.** Force generation in muscle. *Current opinion in cell biology* 2: 62-66, 1990.
- 578 12. **Cooke R.** Modulation of the actomyosin interaction during fatigue of skeletal
579 muscle. *Muscle & nerve* 36: 756-777, 2007.
- 580 13. **Cooke R, Franks K, Luciani GB, and Pate E.** The inhibition of rabbit skeletal muscle
581 contraction by hydrogen ions and phosphate. *The Journal of physiology* 395: 77-97, 1988.
- 582 14. **Coupland ME, Puchert E, and Ranatunga KW.** Temperature dependence of active
583 tension in mammalian (rabbit psoas) muscle fibres: effect of inorganic phosphate. *The*
584 *Journal of physiology* 536: 879-891, 2001.
- 585 15. **Criddle AH, Geeves MA, and Jeffries T.** The use of actin labelled with N-(1-
586 pyrenyl)iodoacetamide to study the interaction of actin with myosin subfragments and
587 troponin/tropomyosin. *The Biochemical journal* 232: 343-349, 1985.
- 588 16. **Debold EP, Beck SE, and Warshaw DM.** Effect of low pH on single skeletal muscle
589 myosin mechanics and kinetics. *American journal of physiology Cell physiology* 295: C173-
590 179, 2008.
- 591 17. **Debold EP, Dave H, and Fitts RH.** Fiber type and temperature dependence of
592 inorganic phosphate: implications for fatigue. *American journal of physiology Cell physiology*
593 287: C673-681, 2004.
- 594 18. **Debold EP, Walcott S, Woodward M, and Turner MA.** Direct observation of
595 phosphate inhibiting the force-generating capacity of a miniensemble of Myosin molecules.
596 *Biophysical journal* 105: 2374-2384, 2013.

- 597 19. **Egan P, Moore J, Schunn C, Cagan J, and LeDuc P.** Emergent Systems Energy Laws
598 for Predicting Myosin Ensemble Processivity. *PLoS Computational Biology* 11: 2015.
- 599 20. **Fabiato A, and Fabiato F.** Effects of pH on the myofilaments and the sarcoplasmic
600 reticulum of skinned cells from cardiac and skeletal muscles. *The Journal of physiology* 276:
601 233-255, 1978.
- 602 21. **Fitts RH.** Muscle fatigue: the cellular aspects. *Am J Sports Med* 24: S9-13.
- 603 22. **Geeves MA.** Review: The ATPase mechanism of myosin and actomyosin.
604 *Biopolymers* 105: 483-491, 2016.
- 605 23. **Green HJ.** Mechanisms of muscle fatigue in intense exercise. *Journal of sports*
606 *sciences* 15: 247-256, 1997.
- 607 24. **Hamada T, Sale DG, MacDougall JD, and Tarnopolsky MA.** Interaction of fibre type,
608 potentiation and fatigue in human knee extensor muscles. *Acta physiologica Scandinavica*
609 178: 165-173, 2003.
- 610 25. **Hamalainen N, and Pette D.** The histochemical profiles of fast fiber types IIB, IID,
611 and IIA in skeletal muscles of mouse, rat, and rabbit. *The journal of histochemistry and*
612 *cytochemistry : official journal of the Histochemistry Society* 41: 733-743, 1993.
- 613 26. **Hancock CR, Brault JJ, and Terjung RL.** Protecting the cellular energy state during
614 contractions: role of AMP deaminase. *Journal of physiology and pharmacology : an official*
615 *journal of the Polish Physiological Society* 57 Suppl 10: 17-29, 2006.
- 616 27. **Hermansen L, and Osnes JB.** Blood and muscle pH after maximal exercise in man. *J*
617 *Appl Physiol* 32: 304-308, 1972.
- 618 28. **Huxley HE, and Hanson J.** The structural basis of the contraction mechanism in
619 striated muscle. *Annals of the New York Academy of Sciences* 81: 403-408, 1959.
- 620 29. **Iorga B, Adamek N, and Geeves MA.** The slow skeletal muscle isoform of myosin
621 shows kinetic features common to smooth and non-muscle myosins. *The Journal of*
622 *biological chemistry* 282: 3559-3570, 2007.
- 623 30. **Johansen KL, Doyle J, Sakkas GK, and Kent-Braun JA.** Neural and metabolic
624 mechanisms of excessive muscle fatigue in maintenance hemodialysis patients. *American*
625 *journal of physiology Regulatory, integrative and comparative physiology* 289: R805-813,
626 2005.
- 627 31. **Juel C, Bangsbo J, Graham T, and Saltin B.** Lactate and potassium fluxes from human
628 skeletal muscle during and after intense, dynamic, knee extensor exercise. *Acta physiologica*
629 *Scandinavica* 140: 147-159, 1990.
- 630 32. **Juel C, Klarskov C, Nielsen JJ, Krstrup P, Mohr M, and Bangsbo J.** Effect of high-
631 intensity intermittent training on lactate and H⁺ release from human skeletal muscle.
632 *American journal of physiology Endocrinology and metabolism* 286: E245-251, 2004.
- 633 33. **Karatzafieri C, Chinn MK, and Cooke R.** The force exerted by a muscle cross-bridge
634 depends directly on the strength of the actomyosin bond. *Biophysical journal* 87: 2532-2544,
635 2004.
- 636 34. **Karatzafieri C, de Haan A, Ferguson RA, van Mechelen W, and Sargeant AJ.**
637 Phosphocreatine and ATP content in human single muscle fibres before and after maximum
638 dynamic exercise. *Pflugers Archiv : European journal of physiology* 442: 467-474, 2001.
- 639 35. **Karatzafieri C, de Haan A, van Mechelen W, and Sargeant AJ.** Metabolic changes in
640 single human fibres during brief maximal exercise. *Experimental physiology* 86: 411-415,
641 2001.
- 642 36. **Karatzafieri C, Franks-Skiba K, and Cooke R.** Inhibition of shortening velocity of
643 skinned skeletal muscle fibers in conditions that mimic fatigue. *American journal of*
644 *physiology Regulatory, integrative and comparative physiology* 294: R948-955, 2008.
- 645 37. **Karatzafieri C, Myburgh KH, Chinn MK, Franks-Skiba K, and Cooke R.** Effect of an
646 ADP analog on isometric force and ATPase activity of active muscle fibers. *American journal*
647 *of physiology Cell physiology* 284: C816-825, 2003.

- 648 38. **Lanza IR, Wigmore DM, Befroy DE, and Kent-Braun JA.** In vivo ATP production
649 during free-flow and ischaemic muscle contractions in humans. *The Journal of physiology*
650 577: 353-367, 2006.
- 651 39. **Macdonald WA, and Stephenson DG.** Effects of ADP on sarcoplasmic reticulum
652 function in mechanically skinned skeletal muscle fibres of the rat. *The Journal of physiology*
653 532: 499-508, 2001.
- 654 40. **Månsson A.** Actomyosin-ADP States, Interhead Cooperativity, and the Force-Velocity
655 Relation of Skeletal Muscle. *Biophysical journal* 98: 1237-1246, 2010.
- 656 41. **Margossian SS, and Lowey S.** Interaction of myosin subfragments with F-actin.
657 *Biochemistry* 17: 5431-5439, 1978.
- 658 42. **Millar NC, and Geeves MA.** The limiting rate of the ATP-mediated dissociation of
659 actin from rabbit skeletal muscle myosin subfragment 1. *FEBS letters* 160: 141-148, 1983.
- 660 43. **Nelson CR, Debold EP, and Fitts RH.** Phosphate and acidosis act synergistically to
661 depress peak power in rat muscle fibers. *American journal of physiology Cell physiology* 307:
662 C939-950, 2014.
- 663 44. **Nyitrai M, Rossi R, Adamek N, Pellegrino MA, Bottinelli R, and Geeves MA.** What
664 limits the velocity of fast-skeletal muscle contraction in mammals? *Journal of molecular*
665 *biology* 355: 432-442, 2006.
- 666 45. **Pate E, Bhimani M, Franks-Skiba K, and Cooke R.** Reduced effect of pH on skinned
667 rabbit psoas muscle mechanics at high temperatures: implications for fatigue. *The Journal of*
668 *physiology* 486 (Pt 3): 689-694, 1995.
- 669 46. **Pate E, and Cooke R.** Addition of phosphate to active muscle fibers probes
670 actomyosin states within the powerstroke. *Pflugers Archiv : European journal of physiology*
671 414: 73-81, 1989.
- 672 47. **Reconditi M, Linari M, Lucii L, Stewart A, Sun YB, Narayanan T, Irving T, Piazzesi G,**
673 **Irving M, and Lombardi V.** Structure-function relation of the myosin motor in striated
674 muscle. *Annals of the New York Academy of Sciences* 1047: 232-247, 2005.
- 675 48. **Sahlin K, Harris RC, Nylinde B, and Hultman E.** Lactate content and pH in muscle
676 samples obtained after dynamic exercise. *Pflügers Archiv* 367: 143-149, 1976.
- 677 49. **Schiaffino S, and Reggiani C.** Fiber types in mammalian skeletal muscles.
678 *Physiological reviews* 91: 1447-1531, 2011.
- 679 50. **Sieck GC, Fournier M, Prakash YS, and Blanco CE.** Myosin phenotype and SDH
680 enzyme variability among motor unit fibers. *Journal of applied physiology* 80: 2179-2189,
681 1996.
- 682 51. **Siemankowski RF, Wiseman MO, and White HD.** ADP dissociation from actomyosin
683 subfragment 1 is sufficiently slow to limit the unloaded shortening velocity in vertebrate
684 muscle. *Proceedings of the National Academy of Sciences of the United States of America* 82:
685 658-662, 1985.
- 686 52. **Spudich JA, and Watt S.** The regulation of rabbit skeletal muscle contraction. I.
687 Biochemical studies of the interaction of the tropomyosin-troponin complex with actin and
688 the proteolytic fragments of myosin. *The Journal of biological chemistry* 246: 4866-4871,
689 1971.
- 690 53. **Tesi C, Colomo F, Nencini S, Piroddi N, and Poggesi C.** The effect of inorganic
691 phosphate on force generation in single myofibrils from rabbit skeletal muscle. *Biophysical*
692 *journal* 78: 3081-3092, 2000.
- 693 54. **Tesi C, Colomo F, Piroddi N, and Poggesi C.** Characterization of the cross-bridge
694 force-generating step using inorganic phosphate and BDM in myofibrils from rabbit skeletal
695 muscles. *The Journal of physiology* 541: 187-199, 2002.
- 696 55. **Toniolo L, Maccatrozzo L, Patrino M, Caliaro F, Mascarello F, and Reggiani C.**
697 Expression of eight distinct MHC isoforms in bovine striated muscles: evidence for MHC-2B

698 presence only in extraocular muscles. *The Journal of experimental biology* 208: 4243-4253,
699 2005.

700 56. **Walklate J, and Geeves MA.** Temperature manifold for a stopped-flow machine to
701 allow measurements from -10 to +40 degrees C. *Analytical biochemistry* 476: 11-16, 2015.

702 57. **Weeds AG, and Taylor RS.** Separation of subfragment-1 isoenzymes from rabbit
703 skeletal muscle myosin. *Nature* 257: 54-56, 1975.

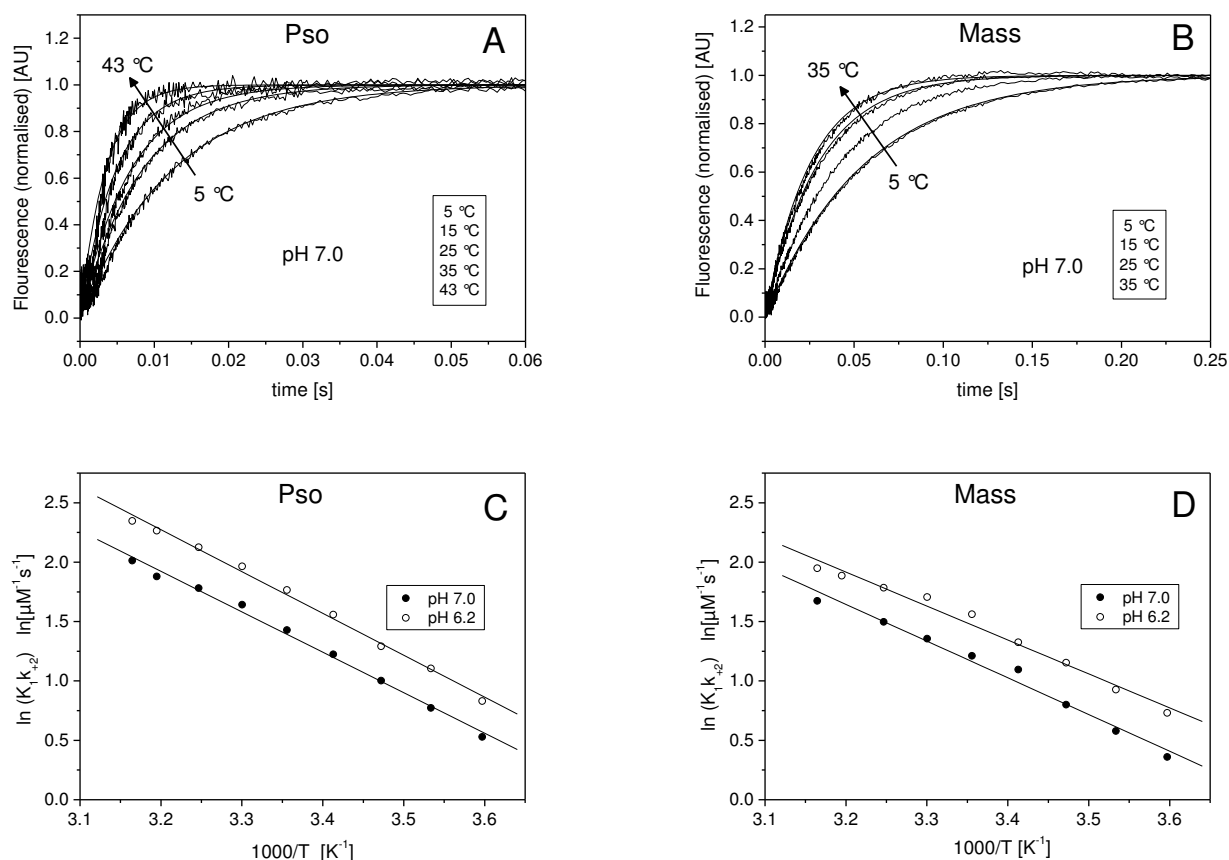
704 58. **Westerblad H, Allen DG, and Lannergren J.** Muscle fatigue: lactic acid or inorganic
705 phosphate the major cause? *News in physiological sciences : an international journal of*
706 *physiology produced jointly by the International Union of Physiological Sciences and the*
707 *American Physiological Society* 17: 17-21, 2002.

708 59. **Westerblad H, Bruton JD, and Lannergren J.** The effect of intracellular pH on
709 contractile function of intact, single fibres of mouse muscle declines with increasing
710 temperature. *The Journal of physiology* 500 (Pt 1): 193-204, 1997.

711

712

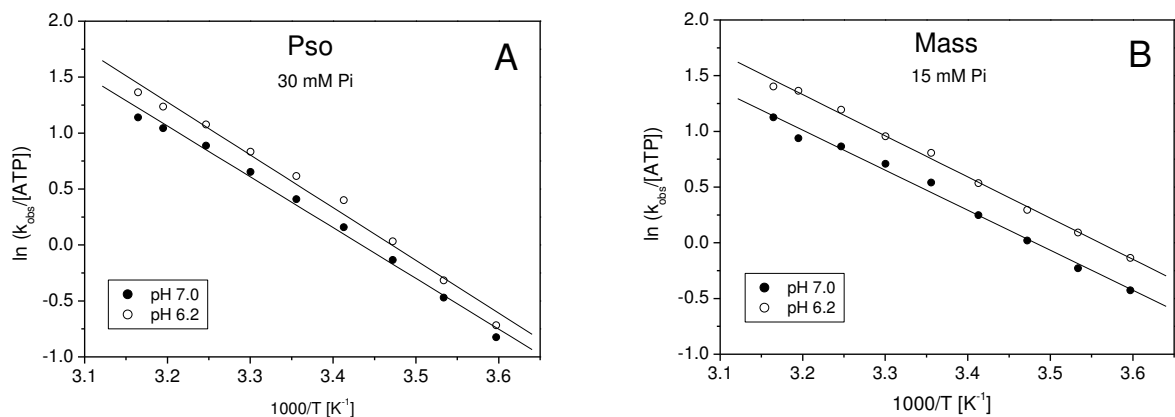
713



715 **Figure 1.** ATP-induced dissociation of S1 from actin, for fast (Pso) and slow (Mass) myosin
 716 isoform, at pH 7.0 and 6.2, in a range of temperatures. A. Normalized transients observed
 717 when mixing 0.5 μM pyr-act.PsoS1 with 25 μM ATP in pH 7.0 buffer at different
 718 temperatures (selected transients are shown). The change in fluorescence was fitted to a
 719 single exponential equation (best fits superimposed), giving k_{obs} of 84.8, 136.2, 208.5, 296.9,
 720 and 374.4 s^{-1} for 5, 15, 25, 35 and 43 $^{\circ}\text{C}$, respectively. The amplitudes of the transients were
 721 relatively stable at 46 % of total fluorescence change, with some loss observed at
 722 temperatures above 30 $^{\circ}\text{C}$. B. Normalized transients observed when mixing 0.5 μM
 723 pyrAct.MassS1 with 25 μM ATP in pH 7.0 buffer at different temperatures (selected
 724 transients are shown). The change in fluorescence was fitted to a single exponential
 725 equation (best fits superimposed), giving observed rate constants of 26.7, 36.1, 46.7, and
 726 64.9 s^{-1} for 5, 15, 25 and 35 $^{\circ}\text{C}$, respectively. The amplitudes of the transients were relatively
 727 stable at 40 % of total fluorescence change, with some loss observed at temperatures above
 728 30 $^{\circ}\text{C}$. C. Arrhenius plot of the $k_{\text{obs}}/[\text{ATP}] = K_1 k_{+2}$ of Pso at pH 7.0 and pH 6.2 (temperature
 729 range 5 – 43 $^{\circ}\text{C}$). The linear fits (best fits superimposed) gave slopes of -3.41 ± 0.10 and -3.52
 730 $\pm 0.09 \text{ K}$ for pH 7.0 and 6.2, respectively, from which the activation energies (E_a) were
 731 calculated as 28.3 ± 0.8 and $29.3 \pm 0.8 \text{ kJ/mol}$. D. Arrhenius plot of the $k_{\text{obs}}/[\text{ATP}] = K_1 k_{+2}$ of
 732 Mass at pH 7.0 and pH 6.2 (temperature range 5 – 43 $^{\circ}\text{C}$). The linear fits (best fits
 733 superimposed) gave slopes of -3.09 ± 0.17 and $-2.86 \pm 0.14 \text{ K}$ for pH 7.0 and 6.2, respectively,
 734 from which the activation energies (E_a) were calculated as 25.7 ± 1.4 and $23.8 \pm 1.1 \text{ kJ/mol}$.

735

736

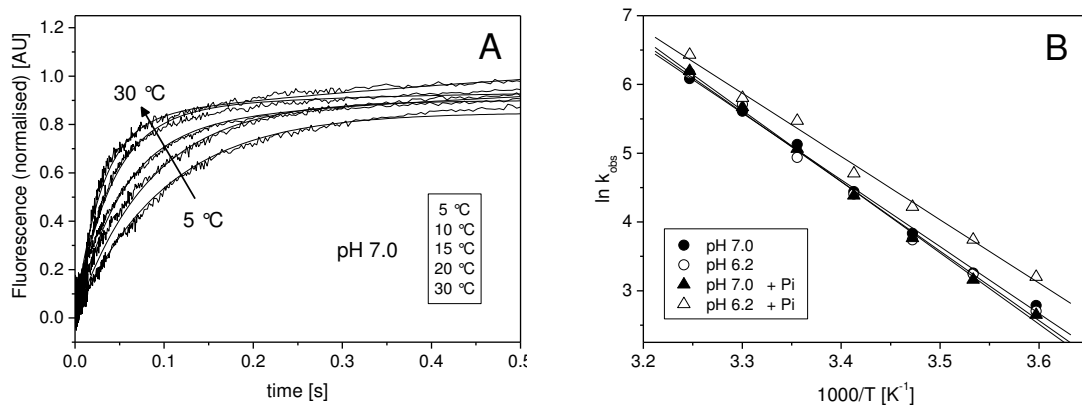


737 **Figure 2.** Effect of inorganic phosphate on the ATP-induced dissociation of S1 from actin, for
738 fast (Pso) and slow (Mass) myosin isoform at pH 7.0 and 6.2, in a range of temperatures. A.
739 Arrhenius plot of the k_{obs} of *Psoas* at pH 7.0 and pH 6.2 in the presence of 30 mM Pi. The
740 linear fits (best fits superimposed) gave slopes of -4.54 ± 0.15 and -4.71 ± 0.20 K for pH 7.0
741 and 6.2, respectively, from which the activation energies (E_a) were calculated as 37.7 ± 1.2
742 and 39.2 ± 1.6 kJ/mol. B. Arrhenius plot of the k_{obs} of *Masseter* at pH 7.0 and pH 6.2 in the
743 presence of 15 mM Pi. The linear fits (best fits superimposed) gave slopes of -3.59 ± 0.13 and
744 -3.694 ± 0.08 K for pH 7.0 and 6.2, respectively, from which the activation energies (E_a) were
745 calculated as 29.9 ± 1.1 and 30.7 ± 0.7 kJ/mol.

746

747

748

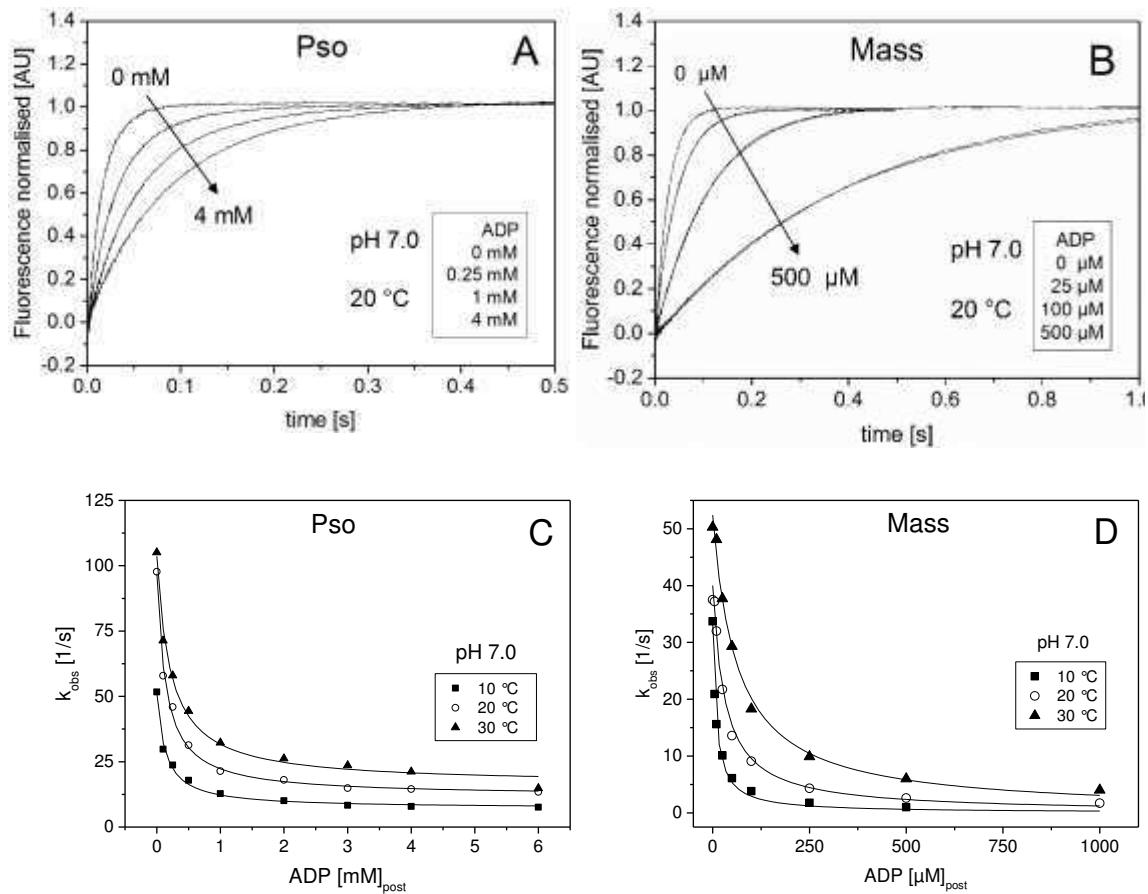


749 **Figure 3.** Temperature dependence of the ADP release from pyrAct.MassS1.A. Normalized
 750 fluorescent transients observed when 0.5 μM pyrAct.MassS1 pre-incubated with 75 μM ADP
 751 was mixed with 8 mM ATP at different temperatures between 5 and 30 $^{\circ}\text{C}$ in pH 7.0 buffer
 752 (selected transients are shown). The change in fluorescence was biphasic when observed
 753 over a time scale of 5 sec, however here only the initial fast phase is shown (fits
 754 superimposed). The k_{obs} for the fast phase were 16.2, 26.0, 46.3, 85.0 and 273 s^{-1} for 5, 10,
 755 15, 20 and 30 $^{\circ}\text{C}$, respectively. B. Arrhenius plot of the k_{obs} of the ADP release rate constant
 756 of *Masseter* at pH 7.0 and pH 6.2 in the absence and presence of 15 mM Pi. The linear fits
 757 (best fits superimposed) gave slopes of -9.72 ± 0.24 and -10.09 ± 0.33 K for pH 7.0 and 6.2,
 758 and -10.36 ± 0.23 and -9.20 ± 0.31 K for pH 7.0+Pi and pH 6.2 +Pi, respectively. The
 759 activation energies (E_a) were calculated as 75.9 ± 4.1 and 84.7 ± 6.1 kJ/mol for pH 7.0 and
 760 6.2 without phosphate, and 94.4 ± 5.0 and 88.9 ± 3.9 kJ/mol for pH 7.0 and pH 6.2
 761 respectively in the presences of phosphate.

762

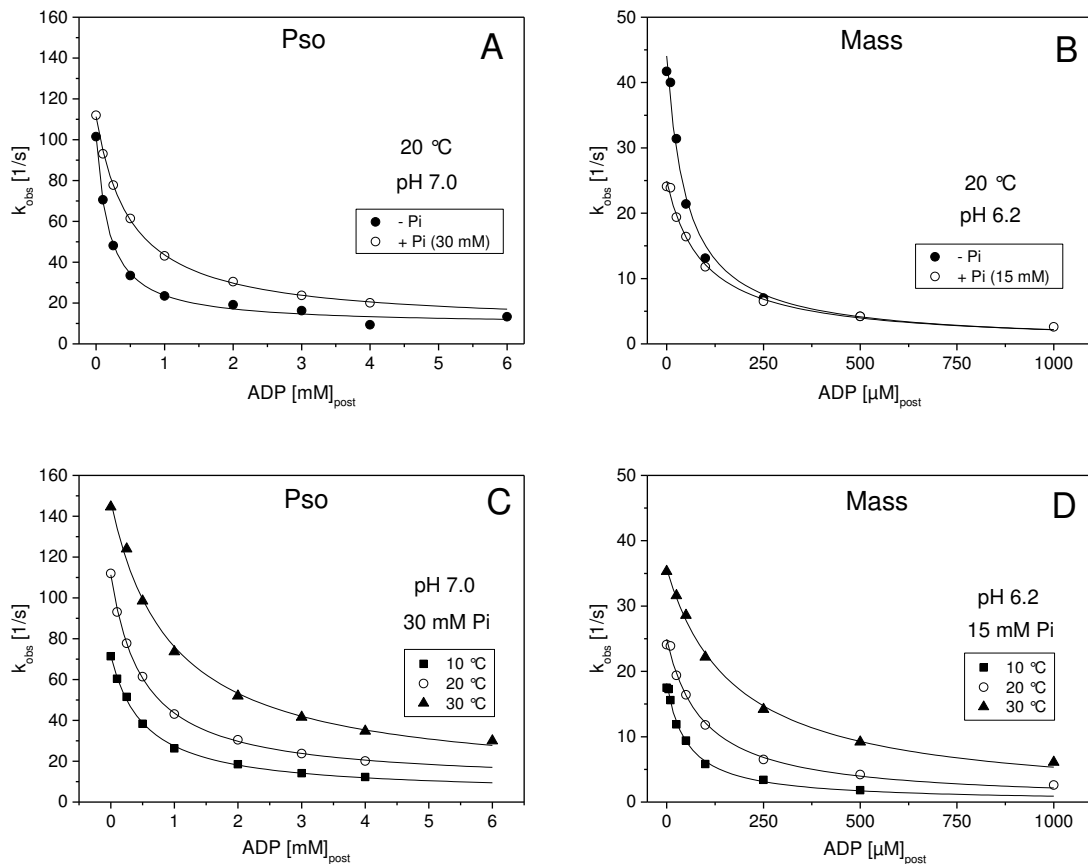
763

764



766

767 **Figure 4.** Temperature dependence of the ADP dissociation constant (K_{ADP}) for fast (Pso) and
 768 slow (Mass) A.S1 at pH 7.0. A. Normalized fluorescent transients observed when 0.5 μM
 769 pyrAct.PsoS1 was mixed with 25 μM ATP with various concentrations of ADP present at 20
 770 $^{\circ}\text{C}$ in pH 7.0 buffer. The change in fluorescence was fitted by a single exponential equation
 771 (best fits superimposed). The k_{obs} determined were 87.7, 45.9, 21.4 and 14.5 s^{-1} for zero,
 772 0.25, 1 and 4 mM ADP, respectively, with an amplitude of 30 % of total fluorescence. B.
 773 Fluorescent transients observed when 0.5 μM pyrAct.MassS1 was mixed with 25 μM ATP
 774 with various concentrations of ADP present at 20 $^{\circ}\text{C}$ in pH 7.0 buffer. The change in
 775 fluorescence was fitted to a single exponential equation (best fits superimposed). The k_{obs}
 776 determined were 37.5, 21.7, 9.1 and 2.6 s^{-1} for zero, 25, 100 and 500 μM ADP, respectively,
 777 with an amplitude of 30 % of total fluorescence. C. Plot of the observed rate constants as a
 778 function of [ADP] for *Psoas* in pH 7.0 buffer at 10, 20 and 30 $^{\circ}\text{C}$. The data sets were fitted to
 779 a hyperbole to obtain the ADP dissociation constant (K_{ADP}) for each temperature: 131 ± 16
 780 μM (10 $^{\circ}\text{C}$), $140 \pm 14 \mu\text{M}$ (20 $^{\circ}\text{C}$) and $213 \pm 29 \mu\text{M}$ (30 $^{\circ}\text{C}$) for the depicted data. Refer to
 781 Table 1 for average values for from measurements in different days. D. Plot of the observed
 782 rate constants as a function of [ADP] for *Masseter* in pH 7.0 buffer at 10, 20 and 30 $^{\circ}\text{C}$. The
 783 data sets were fitted to a hyperbole to obtain the ADP dissociation constant (K_{ADP}) for each
 784 temperature: $9.6 \pm 0.7 \mu\text{M}$ (10 $^{\circ}\text{C}$), $31.3 \pm 4.0 \mu\text{M}$ (20 $^{\circ}\text{C}$) and $62.4 \pm 6.1 \mu\text{M}$ (30 $^{\circ}\text{C}$) for the
 785 depicted data. Refer to Table 1 for average values from measurements in different days.

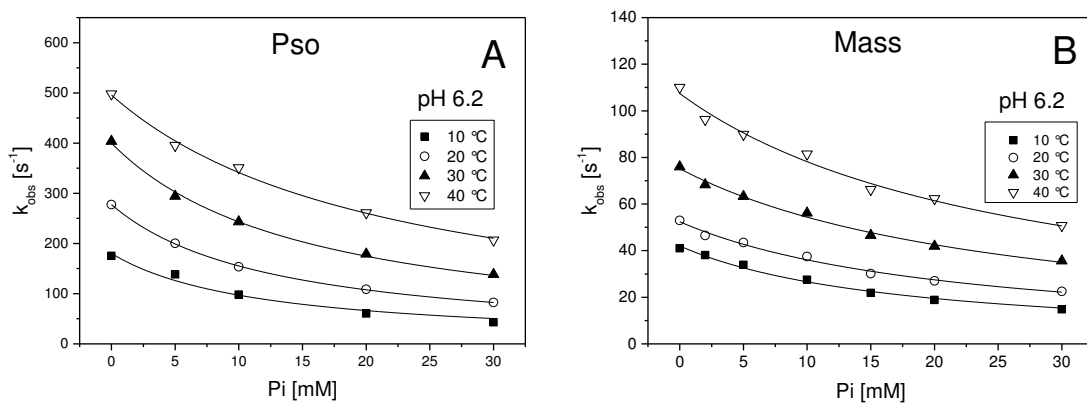


787 **Figure 5.** Effect of phosphate (Pi) on the K_{AD} of fast (*Pso*) and slow (*Mass*) A.S1. A. Plot of the
 788 observed rate constants as a function of [ADP] for *Psoas* in the presence and absence of
 789 added 30 mM Pi (pH 7.0 buffer at 20 °C). The data sets were fitted to a hyperbole to obtain
 790 the ADP dissociation constant ($K_{\text{ADP}} \pm \text{Pi}$): $175 \pm 22 \mu\text{M}$ (no Pi) and $510 \pm 22 \mu\text{M}$ (with Pi).
 791 Refer to Table 1 for average values for from measurements in different days. B. Plot of the
 792 observed rate constants as a function of [ADP] for *Masseter* in the presence and absence of
 793 added 15 mM Pi (pH 6.2 buffer at 20 °C). The data sets were fitted to a hyperbole to obtain
 794 the ADP dissociation constant ($K_{\text{ADP}} \pm \text{Pi}$): $48.4 \pm 6.8 \mu\text{M}$ (no Pi) and $94.5 \pm 8.1 \mu\text{M}$ (with Pi).
 795 Refer to Table 1 for average values for from measurements in different days. C. Plot of the
 796 observed rate constants as a function of [ADP] for *Psoas* in pH 7.0 buffer in the presence of
 797 added 30 mM Pi at 10, 20 and 30 °C. The data sets were fitted to a hyperbole to obtain the
 798 ADP dissociation constant (K_{ADP}) for each temperature: $530 \pm 36 \mu\text{M}$ (10 °C), $510 \pm 22 \mu\text{M}$ (20
 799 °C) and $942 \pm 117 \mu\text{M}$ (30 °C). Refer to Table 1 for average values for from measurements in
 800 different days. D. Plot of the observed rate constants as a function of [ADP] for *Masseter* in
 801 pH 6.2 buffer in the presence of added 15 mM Pi at 10, 20 and 30 °C. The data sets were
 802 fitted to a hyperbole to obtain the ADP dissociation constant (K_{ADP}) for each temperature:
 803 $52.2 \pm 5.8 \mu\text{M}$ (10 °C), $94.5 \pm 8.1 \mu\text{M}$ (20 °C) and $175.3 \pm 9.7 \mu\text{M}$ (30 °C). Refer to Table 1 for
 804 average values for from measurements in different days.

805

806

807



808

809 **Figure 6.** Phosphate (Pi) dissociation constant for A.M in the absence of ADP (phosphate) at
 810 pH 6.2, for fast (Pso) and slow (Mass) myosin isoform. A. Plot of the observed rate constants
 811 of the ATP-induced dissociation of 0.5 μM pyrAct.S1 by 50 μM ATP as a function of [Pi] for
 812 *Psoas* (pH 6.2 buffer) at 10 to 40 $^{\circ}\text{C}$. The data sets were fitted to a hyperbole to obtain the Pi
 813 dissociation constant (K_{pi}) for each temperature: 11.7 ± 1.8 mM (10 $^{\circ}\text{C}$), 12.7 ± 0.2 mM (20
 814 $^{\circ}\text{C}$), 15.5 ± 0.7 mM (30 $^{\circ}\text{C}$) and 22.1 ± 1.2 mM (40 $^{\circ}\text{C}$). Refer to Table 1 for average values for
 815 from measurements in different days. B. Plot of the observed rate constants of the ATP-
 816 induced dissociation of 0.5 μM pyrAct.S1 by 25 μM ATP as a function of [Pi] for *Masseter* (pH
 817 6.2 buffer) at 10 to 40 $^{\circ}\text{C}$. The data sets were fitted to a hyperbole to obtain the Pi
 818 dissociation constant (K_{pi}) for each temperature: 17.3 ± 1.1 mM (10 $^{\circ}\text{C}$), 22.0 ± 1.4 mM (20
 819 $^{\circ}\text{C}$), 26.1 ± 1.3 mM (30 $^{\circ}\text{C}$) and 26.7 ± 2.1 mM (40 $^{\circ}\text{C}$). Refer to Table 1 for average values for
 820 from measurements in different days.

821

822

823

824

825

826

827 **Tables**

828 **Table 1.** Average values of kinetic parameters describing the ATP induced
829 dissociation rate of actin.S1 for psoas and masseter myosin, in pH 7 and 6.2, under
830 different temperatures, in the absence or presence of added phosphate.

831

832

833

834

835 **Table 2.** Thermodynamics results (E_A values) describing the temperature
836 dependence of the dissociation rate constant for psoas (Pso) and masseter (Mass)
837 myosin, under pH 7 and 6.2.

838

839

840

Modulators of actin-myosin dissociation: basis for muscle type differences in contraction during fatigue

104 characters incl. spaces

Authors: Christina Karatzaferi^{1,2}, Nancy Adamek³, and Michael A. Geeves³

¹ Muscle Physiology and Mechanics Group, DPESS, University of Thessaly, Karyes, Trikala, 42100, Greece

² Experimental Myology and Integrative Biology Cluster, FSHS, University of St Mark and St John UK

³ School of Biosciences, University of Kent, Canterbury, CT2 7NH Kent, UK

Running head: Muscle type actomyosin dissociation differences in fatigue

58 characters incl. spaces

Address for correspondence: M.A. Geeves, School of Biological Sciences, University of Kent, Canterbury, CT2 7NH Kent, UK M.A.Geeves@kent.ac.uk

Author contributions: CK & MAG conceived the study, MAG & CK designed the study, NA & CK collected data, NA created figures and tables, all co-wrote and edited the paper.

Abstract

The muscle types present with variable fatigue tolerance, in part due to the myosin isoform expressed. However, the critical steps that define 'fatigability' *in vivo* of fast vs slow myosin isoforms, at the molecular level, are not yet fully understood. We examined the modulation of the ATP-induced myosin sub-fragment 1 (S1) dissociation from pyrene-actin by inorganic phosphate (Pi), pH and temperature using a specially modified stopped-flow system (HiTech Scientific SF-61DX2) that allowed fast kinetics measurements at physiological temperature. We contrasted the properties of rabbit psoas (fast) and bovine masseter (slow) myosins (obtained from samples collected from New Zealand rabbits and from a licensed abattoir, respectively, according to institutional and national ethics permits). To identify ATP cycling biochemical intermediates, we assessed ATP binding to a pre-equilibrated mixture of actomyosin and variable [ADP], pH (pH 7 vs pH 6.2) and Pi (zero, 15 or 30 added mM Pi) in a range of temperatures (5 to 45°C). Temperature and pH variations had little, if any, effect on ADP affinity (K_{ADP}) for fast S1 but for slow S1 K_{ADP} was weakened with increasing temperature or low pH. In the absence of ADP, affinity for phosphate (K_{Pi}) was weakened with increasing temperature for fast S1. In the presence of ADP, myosin type differences were revealed at the apparent phosphate affinity, depending on pH and temperature. Overall, the data point to distinct mechanochemical coupling differences between myosin types which could help explain the *in vivo* observed muscle types differences at rest and during fatigue.

248 words

Keywords: myosin kinetics, cross-bridge cycle, mechanochemical coupling, temperature, muscle fatigue

Introduction

Mammalian striated muscle contraction depends directly on the interaction of the motor protein myosin II, organized in multi-headed filaments, with the filamentous 'tracks' of actin, all arranged along with other proteins into sarcomeres, the 'functional units' of muscle (23, 38). In essence whole muscle force output eventually depends on the number of myosin cross bridges interacting 'strongly' or 'weakly' with actin, while the velocity of contraction depends on the rate at which myosin detaches from actin at the end of the working stroke (8).

Peripheral muscle fatigue is manifested by a transient reduction in work or power output induced by physical exertion. Depression of muscle power comes as a result of force decline and the slowing of contraction velocity and is accompanied by biochemical alterations of the intracellular milieu (9, 18). Because the decline in force can be accompanied by a relatively larger reduction of energy turnover (i.e. tension economy, observed in *in situ* (19) or isolated intact muscle models (13), fatigue could be also viewed as a physiological protective mechanism 'saving' the tissue from a potential energetic crisis. At the organismal level, fatigue is revealed to be a complex multifaceted phenomenon, with a large heterogeneity of research outcomes (4) depending, among other factors, on the type, duration and intensity of muscular activity employed (5, 7), the muscle composition studied (22) and health status (25). Still, recovery of the muscle's performance capacity is observed with adequate rest, this being a 'criterion' of physiological peripheral fatigue. At the muscle cellular level, changes in muscle mechanics during fatigue could be related to either reduction of energy substrates (e.g. causing localized ATP minima (27, 28)) and /or accumulation of ATP hydrolysis by-products (e.g. (11, 26, 30, 36, 43)). This is because the interaction of myosin with actin (actomyosin) is not only fueled by ATP hydrolysis but it is also modulated by ATP hydrolysis by-products (ADP, Pi, H⁺) and other prevailing intracellular conditions (9). Thus, at the myofibrillar level, and for the purposes of this work, fatigue is considered in the context of factors influencing the actomyosin cycle in a way to cause slowing of the cycle and/or weaker actomyosin interactions.

The coupling of biochemical steps with mechanical events has, however, not been fully elucidated (20) while the 'laws' governing how large ensembles of myosins integrate within the organized sarcomere (16, 17, 31) are not yet fully defined. Investigations ranging from whole body exercise (5, 25), to intact small muscles or fibers (48) to skinned fibers, (10, 11, 15, 26, 30, 37) or myofibrils (43), and isolated molecule approaches (14) have provided strong evidence that the accumulation of inorganic phosphate (Pi) and of hydrogen ions can contribute to, if not cause, peripheral muscle fatigue. Still, their exact impact, especially at physiological *in vivo* conditions, has attracted much debate (e.g. (47)). This is further complicated by muscle type differences (fast vs slow) in energetics, myosin ATPase, and mechanical performance (6, 39, 40) , which can be linked to a great degree to inherent properties of the myosin II isoform expressed.

Myosin II exists in multiple isoforms (39) with *slow* muscles expressing the type 1 (MyHC-1 also known as β myosin) and *fast* muscles expressing one or more of the type 2 myosins (MyHC-2a, 2b, or 2x). The study of kinetics of the actomyosin (A.M) interaction cycle identifies clear intermediate steps (for a review see (3)). Such studies have revealed that slow skeletal myosin heavy chain isoforms (MyHC 1) have distinct properties from fast isoforms (MyHC 2s) with regards not only to the ATPase activity but also to the rate and equilibrium constants of the various biochemical steps of the pathway which are expected to dictate their different mechanical properties. For example, efficiency of actin induced ADP displacement from myosin (the ratio of ADP affinity for A.M (K_{AD}) over the ADP affinity for myosin (K_D)), and strain sensitivity (dependence on external mechanical load) can differ substantially between fast and slow myosins (3, 20) , with slow myosins binding ADP tightly and releasing it at a slower rate than fast myosins. Thus, it is considered that the ADP release is the rate limiting step for the maximum contraction velocity of slow muscles (24, 35), at least at the temperatures where fibers or myosin solutions are usually studied (10 to 22 °C).

However, *in vivo* mammalian muscle temperature ranges from 32 to > 40 °C, while in severe fatigue, pH drops and inorganic phosphate (Pi) accumulates (21). A number of *in vitro* fiber studies at higher temperatures, have challenged long held views about

the individual role of the key 'fatigue' metabolites on mechanics, e.g. low pH on force (less of an effect (29, 36, 48)), high Pi on force (less of an effect, (10, 11, 15, 26)). More importantly, it appears that a higher temperature is necessary to tease out physiological synergies; e.g. in skinned fibers, a synergism of myosin light chain phosphorylation with low pH and high [Pi] in slowing contraction velocity and repressing power output became evident only in experiments performed at a high temperature (29) . Overall, many studies now indicate that temperature considerations and a holistic, systems, approach are crucial if one wants to realistically link muscle function *in vivo* to actomyosin interaction molecular events studied *in vitro*.

The steps that control the detachment of the myosin cross-bridge at the end of the working stroke from actin are rapid and are thought to limit the shortening velocity, a key parameter of muscle function. Temperature predictions from kinetic studies of actomyosin in solution (35), suggest that the rate of ADP release may limit unloaded velocity for both isoforms. It can be hypothesized that such an ADP effect could be aggravated by the presence of hydrogen ions and inorganic phosphate, as in fatigue.

Therefore the purpose of this research was to study the fast kinetics of ATP-induced dissociation of A.M. with and without ADP using the stopped flow. We examined the interplay of 'fatigue' factors, e.g. low pH and high inorganic phosphate (Pi), with myosin type, on ATP-induced dissociation of A.M. Taking advantage of recent methodological advancements we studied, for the first time, the ATP-induced dissociation of fast and slow S1 from actin in temperatures ranging from 5 to 45 °C to reveal critical myosin type and/or temperature dependencies of these processes.

Glossary & abbreviations

A.M: actomyosin complex

S1: myosin subfragment 1

actin.S1: actin bound with S1

K_1 : equilibrium constant for the formation of the complex of AM with ATP (denoted as A.M.T),

k_{+2} : rate constant of isomerization of A.M.T to A-M.T which is followed by actin dissociation

k_{obs} : observed rate constant of ATP induced dissociation of myosin from actin

K_{ADP} : affinity for ADP

K_{Pi} : affinity for phosphate

$K_{\text{ADP+Pi}}$: affinity for ADP in the presence of phosphate

MyHC: myosin heavy chain

Materials and methods

Ethics Statement

Muscle tissue was obtained post-mortem from animals treated as recommended by national and local guidelines (UK Animals (Scientific Procedures) Act, 1986). Fast skeletal muscle came from the psoas muscle of New Zealand rabbits and slow skeletal muscle from bovine masseter.

Protein preparation

Myosin was prepared from the rabbit psoas (for fast MyHC-II) and the bovine masseter muscle (for slow MyHC-I) according to Margossian and Lowey (32), and was subsequently digested to subfragment 1 (S1) with chymotrypsin as described by Weeds & Taylor (46). Actin was prepared from rabbit muscle as described by Spudich & Watt (42) and labelled with pyrene iodoacetamide to give pyrene-labelled actin as described by Criddle et al (12). Protein stocks of S1 and of pyrene-labelled actin were stored at 4°C and were used for up to 2 weeks. In the text herein reference to actin implies pyrene-labelled actin.

Experimental buffers

The main buffer contained 20 mM cacodylate (adjusted at pH 7.0 or pH 6.2), 100 mM KCl, 5 mM MgCl₂ and 1 mM NaN₃; when phosphate was present in the buffer the ionic strength was adjusted accordingly to a final ionic strength of 170 mM. Concentrations (whether of proteins or buffer constituents) given in the text and figure legends refer to the concentration after mixing 1:1 in the stopped flow (unless stated otherwise).

Experimental equipment and procedures

Stopped-flow experiments were performed essentially as described previously (2) using a HiTech Scientific SF-61DX2 stopped flow system and 4-5 transients were acquired for each ATP transients (Kinetic Studio suite). The dead time of the equipment was 0.002 s. A wide temperature range (5 – 45 °C) for measurements was available because of a new adaptation of the standard stopped flow machine (see (45)). Briefly, the drive syringes were held at room temperature (20 °C) while loading lines leading into the mixing chamber, the mixing and observation chamber were all thermostated at the temperature of the measurement. Essentially the samples were only exposed to the temperature of the measurement for a few seconds, thus allowing measurements of proteins under conditions where they are not usually stable for long.

The **ATP induced dissociation rate of actin.S1**, was measured in the stopped-flow by mixing a fixed concentration of pyr.actin.S1 complex (end concentration 0.25 μM) with excess ATP and monitoring fluorescence transients from the pyrene-labeled actin (excitation at 365 nm, emission through a KV389 nm cut-off filter (Schott, Mainz, Germany)).

In a similar process, **ADP affinity** (K_{ADP}) was measured by adding ADP as a competitive inhibitor of ATP. In this case 0.5 μM pyr.actin.S1 was mixed with 25 μM ATP with various concentrations of ADP present with the ATP (from 0 to 1200 μM).

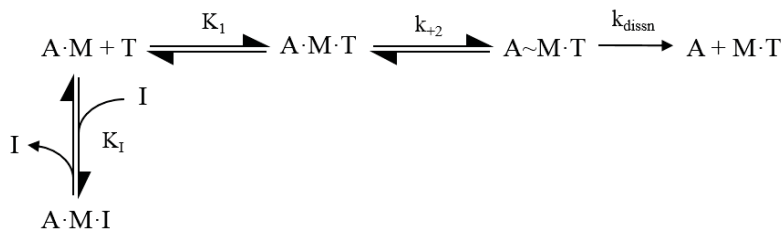
Phosphate affinity (K_{Pi}) was measured exactly as for the ADP affinity except that the high concentrations of P_i used meant it was more convenient to have P_i present in the buffer in both syringes of the stopped-flow.

ADP affinity in the presence of phosphate ($K_{\text{ADP+Pi}}$) was also measured using the same approach as for K_{ADP} but using buffers containing fixed amounts of inorganic phosphate, 30 mM in the case of psoas S1 and 15 mM with masseter S1. The different affinities of P_i for the two types of S1 required a different concentration of P_i .

Experiments were performed at two pH levels, 7 and 6.2 and in a range of temperatures. Care was taken to reverse the order of experiments to avoid the possibility of a time and 'order' effect either with respects to pH or temperature.

Data Fitting and Interpretation Approach

In the present study we focused our attention on the ATP induced dissociation of actin.S1. This is the step that controls the detachment of the actomyosin cross-bridge at the end of the working stroke.



Scheme 1. Model of ATP-induced dissociation of actin.S1 based on Millar and Geeves (33) .

In Scheme 1, T = ATP; A = actin; M = myosin; I is an inhibitor, competitive with ATP for the nucleotide binding site. K_1 defines the equilibrium constant for the formation of the A.M.T collision complex, which is followed by an almost irreversible isomerization of the complex to the ternary complex A-M.T with the rate constant of k_{+2} . This is rapidly followed by dissociation of actin from the ternary complex. K_i is defined as a dissociation constant k_{+i}/k_{-i} . In the experiments presented here the inhibitor was either ADP or inorganic phosphate (P_i).

The reaction described in Scheme 1 was monitored through pyrene fluorescence changes which monitor the ATP induced dissociation of actin from the complex (fluorescence increases by up to 70 %.), specifically associated with step 2 of Scheme 1, (see in Results, Fig. 1A). Four to five transients were collected for each ATP concentration used then averaged before further analysis.

The averaged transients were fitted with single (eqn1) or, if needed, a double exponential equation (eqn2):

$$F_t = \Delta F \cdot e^{(-k_{obs}t)} + F_\infty \quad eqn 1$$

or

$$F_t = \Delta F_{(1)} \cdot e^{(-k_{obs(1)}t)} + \Delta F_{(2)} \cdot e^{(-k_{obs(2)}t)} + F_\infty \quad eqn 2$$

Where F_t is the observed fluorescence at time t , F_∞ is the fluorescence at the end of the transient ($t = \infty$) and ΔF is the total change of fluorescence observed. The observed rate constant (k_{obs}) reflects the ATP induced dissociation rate of actin.S1 and is linearly dependent on $[ATP]$, at the ATP concentrations used here. A plot of $[ATP]$ vs k_{obs} was used to derive the values of K_1 and k_{+2} (using Origin v 6.0), as defined in scheme 1 and eqn 3.

$$k_{obs} = K_1 k_{+2} [ATP] \quad eqn 3$$

The presence of a competitive inhibitor to ATP binding (that does not induce actin.S1 dissociation) would appear to slow the rate of actin.S1 dissociation. If inhibitor binding is in rapid equilibrium with actin.S1, within the timescale of data acquisition, compared to the rate of ATP-induced dissociation of actin.S1 (i.e. $k_{+AD} + [ADP]k_{-AD} \gg K_1 k_{+2} [ATP]$), then

$$k_{obs} = K_1 k_{+2} [ATP] / (1 + ([ADP]/K_i)) \quad eqn 4$$

Then, plotting k_{obs} as a function of $[I]$ will allow the K_i (in scheme 1) to be defined. This approach was used to define the value of K_i for ADP (K_{AD}) and Pi (K_{Pi}).

If both ADP and Pi are present in the same measurement, two scenarios are possible. If both compete for the same binding site then the effect of the two inhibitors is additive and the effect on k_{obs} can be predicted from the values of K_{AD} and K_{Pi} measured independently.

$$k_{obs} = K_1 k_{+2} [ATP] / (1 + ([ADP]/K_{AD}) + ([Pi]/K_{Pi})) \quad eqn 5$$

where the measured K_i at fixed $[Pi]$ as in $K_i = 1/K_{AD} + [Pi]/K_{Pi}$

If both however bind into the ATP pocket at the same time to create the complex A.M.ADP.Pi then the above relationship will not hold and Pi will alter the affinity of

A.M for ADP.

The apparent affinity of ADP for actin.S1 ($K_{ADP.Pi}$) was measured for several concentrations of Pi and then the affinity of Pi calculated according to the following relationship and compared with the value of K_{Pi} .

$$K_{Pi\ app} = [Pi]/(K_{ADP+Pi}/K_{ADP} - 1) \quad \text{eqn 6}$$

ADP release rate constant. Two types of myosins were studied which are known to differ in their affinity for nucleotides (3, 41). The rate constant for the release of ADP (k_{ADP}) is relatively slow and can easily be measured in an ADP displacement experiment. This step is very fast for a fast muscle isoform and too fast to measure by current equipment. Briefly, actin.^{Mass}S1 saturated with 75 μ M of ADP (A.M.D complex) was mixed with a large excess of ATP (8 mM) in the stopped-flow. Then the k_{obs} values, fitted to a single exponential equation (eqn 1) defined the rate constant by which ADP is released by the ternary A.M.D complex (k_{AD}).

The data presented in the figures are the values for the individual experiment displayed, while the data values presented in the table 1 are averaged values for n = independent day measurements.

The *temperature dependence* of the above studied biochemical steps K_1k_{+2} , K_{AD} , K_{Pi} and $K_{ADP.Pi}$ data were plotted as the natural logarithm of the measured parameter against the reciprocal of temperature in degrees Kelvin ($1/T$ °K) and fitted with linear regression using the Arrhenius (rate constants) or vant Hoff (equilibrium constants) equations

$$\ln K_1k_{+2} = \ln(A) - E_a/RT \quad \text{eqn 7}$$

$$\ln K_{eq} = \Delta S^\circ/R - \Delta H^\circ/RT \quad \text{eqn 8}$$

where E_a stands for activation energy, R is the gas constant, A is a pre-exponential factor. The values of $-E_a/R$ or $\Delta H^\circ/R$ were derived from the slopes.

Results & Discussion

ATP induced dissociation rate of actin.S1. When Actin.^{Pso}S1 and actin.^{Mass}S1 were mixed with ATP, as shown in Figure 1 A and B, the observed stopped-flow transients were described by a single exponential for both myosin isoforms (Fig 1A and 1B). Keeping a fixed ATP concentration and increasing the temperature allows the best estimate of the temperature dependence of the reaction since it minimizes variation in ATP concentration between experiments. Increasing the temperature from 5-43 °C reduced the total fluorescence signal by ~ 40% due to collisional quenching but the signal change remained relatively constant with an approximately 2-fold increase in fluorescence observed in all transients. The transients were therefore normalized to illustrate the change in the k_{obs} values. For *psoas* (Fig 1 A) and *masseter* (Fig 1 B) temperature increased the k_{obs} value ~3 fold in both cases over the range of measurements from 3 to 43 °C. The figure shows illustrative examples of one set of transients.

Lowering the pH to 6.2 slightly increased the k_{obs} values for both isoforms by about 20-25 % (and hence the second order rate constant K_1k_{+2} , see Table 1). Increasing temperature resulted in an average increase of 3 fold over the temperature range of 5-35 °C. The amplitudes of the transients at pH 6.2 were again relatively stable and similar to pH 7 for ^{Pso}S1 at 43 %. For ^{Mass}S1 the amplitudes were also stable in pH 6.2 but showed an overall increase in fluorescence from 40 to 50% of total fluorescence signal.

Effect of temperature: The temperature dependence of the dissociation rate constant was examined at pH 7 and then repeated at pH 6.2 (Fig 1C and 1D). Each measurement was repeated 3 times and the average values collated in Table 2. The Arrhenius plots of the temperature dependence measurements at pH 7 and 6.2 gave well defined straight lines over the temperature range (5 – 43 °C). In the absence of phosphate, for *psoas* the activation energy (E_a) values were very similar at pH 7.0 and 6.2 as shown in Figure 1 C, 28.3 ± 0.8 and 29.3 ± 0.8 kJ/mol respectively. For *masseter*, E_a values were on average lower than the ones for fast, being for pH 7.0 and 6.2, 25.7 ± 1.4 and 23.8 ± 1.1 kJ/mol respectively (Figure 1D).

Effect of Pi and pH: When the ATP-induced dissociation measurements were repeated in the presence of high phosphate concentrations, of the order that might be expected in fatigue, the observed rate constants for the dissociation reaction were 2-fold slower for $^{Mass}S1$ and 2- to 3-fold slower for $^{Pso}S1$ at both pH levels compared to the data in the absence of phosphate. This is consistent with Pi acting as a competitive inhibitor with a K_i of 10 – 20 mM. It should be noted that while 30 mM Pi was used for $^{Pso}S1$, 15 mM Pi was used for $^{Mass}S1$ experiments.

The transients of both isoforms had bi-phasic tendencies at the low temperatures (5-10 °C) at both pHs, but were single exponential at all other temperatures. The origin of this additional slow phase, which had a very small amplitude (1-3 %), is not known, but possible contamination by ADP was eliminated by control measurements in the presence of apyrase.

The amplitudes of the dissociation reaction were 50 % smaller/reduced in the presence of phosphate for both, $^{Pso}S1$ and $^{Mass}S1$, indicating some loss of affinity of S1 for actin in the presence of Pi. However, for *psoas* the amplitudes increased with temperature from 25 to 30 % at pH 7.0 and even more dramatically from 12 to 20 % at pH 6.2. This behavior was not observed with $^{Mass}S1$ *masseter*.

Combined effect of temperature, pH and phosphate: the temperature dependence of the dissociation rate constant in the presence of phosphate is shown in Figure 2 and the activation energies determined for *psoas* (38 ± 1 kJ/mol) and *masseter* (30 ± 1 kJ/mol) were greater than in the absence of Pi, irrespective of the pH used. Thus phosphate increased the activation energy of $^{Pso}S1$ at both pH values by about 10 kJ/mol, which is a larger increase than observed with *masseter*, where the increase was only about 5 kJ/mol in the presence of phosphate.

Rate constant of ADP release (k_{ADP}) was evaluated by an ADP displacement experiment, mixing actin. $^{Mass}S1$ saturated with ADP with an excess of ATP. This measurement was not possible for $^{Psoas}S1$ because the ADP release is too fast to measure.

Displacement of ADP from actin.^{Mass}S1 by a large excess of ATP was biphasic. The transients were well-defined with stable amplitudes of 24 and 6 % for the fast and slow phase, respectively (as shown in Figure 3 A). These amplitudes were similar under all conditions explored. The fast phase defines the rate constant at which ADP is released and is thought to limit the velocity of shortening of a masseter muscle (2). The slower phase is an off pathway event and will not be considered further here. The k_{obs} of the ADP release was 85 s^{-1} at $20 \text{ }^{\circ}\text{C}$ (pH 7.0) and compares well to published results of 94 s^{-1} by Bloemink et al (2).

The reaction was measured over the temperature range of $5 - 30 \text{ }^{\circ}\text{C}$ at pH 6.2 and 7.0, and in the presence of 15 mM Pi. The k_{obs} values are summarized in the Arrhenius plot in Fig 3B. The k_{obs} values increased from 16.2 at $5 \text{ }^{\circ}\text{C}$ to 273 s^{-1} at $30 \text{ }^{\circ}\text{C}$ with similar values at pH 7.0 and pH 6.2 throughout the temperature range used. Above $30 \text{ }^{\circ}\text{C}$ the reaction was too fast to measure reliably. Thus the activation energy was large with similar values at both pH levels studied.

The addition of 15 mM Pi had little effect at pH 7.0. At pH 6.2 however we saw a 30-50 % increase in k_{obs} in the presence of phosphate and a small change in the activation energy.

ADP affinity (K_{ADP})

The ADP affinity (K_{ADP}) for pyr.actin.S1 was measured by the competitive inhibitor approach as described in the Methods.

ADP included in the ATP solution competes with ATP for binding to the pyr.actin.S1 and slows the k_{obs} value as shown in Fig 4. The ADP affinity was $168 \text{ }\mu\text{M}$ for ^{Pso}S1 and $31 \text{ }\mu\text{M}$ for ^{Mass}S1 at $20 \text{ }^{\circ}\text{C}$ and pH 7.0, as reported previously²². This large difference in the affinity of actin.S1 for ADP is a major characteristic of a fast vs a slow myosin isoform. As reported previously the ADP affinity for *psoas* actin.S1 was relatively unaffected by temperature (about $200 \pm 30 \text{ }\mu\text{M}$ between 10 and $30 \text{ }^{\circ}\text{C}$) while for

masseter the effect was much greater, with the affinity becoming weaker by ~6-fold from 9.6 μM at 10 $^{\circ}\text{C}$ to 62.4 at 30 $^{\circ}\text{C}$, at pH 7.0.

Effect of pH: A change in pH did not affect the ADP affinity for *psoas* (Table 1) over the temperature range studied (also Figure 4C). Lowering the pH to 6.2 with ^{Mass}S1 resulted in 2-fold weaker K_{AD} values than at pH 7.0 (from 10 to 22 μM at 10 $^{\circ}\text{C}$). However, this effect of pH was not as pronounced at higher temperatures (only weakening by 1.5 fold at 30 $^{\circ}\text{C}$, see Table 1).

Phosphate affinity (K_{Pi})

The affinity of Pi for actin.S1 (K_{Pi}) was measured but the range of Pi concentrations accessible was restricted by the need to maintain a constant ionic strength. As Pi was increased the concentration of KCl in the buffer was decreased and the maximum phosphate concentration used was 30 mM. Figure 6 shows the plots of k_{obs} as a function of phosphate concentration for the two myosin isoforms. These show the expected inhibition as [Pi] is increased with an average K_{Pi} value of 15 mM at 10 $^{\circ}\text{C}$ decreasing to 41 mM at 40 $^{\circ}\text{C}$ for actin.^{Pso}S1 at pH 7.0. Decreasing the pH to 6.2 did not significantly affect the K_{Pi} values for ^{Pso}S1 (11 mM at 10 $^{\circ}\text{C}$, decreasing to 32 mM at 40 $^{\circ}\text{C}$, see also Table 1).

Repeating the measurements with ^{Mass}S1 gave a K_{Pi} of 22 mM at 10 $^{\circ}\text{C}$, weakened to 35 mM at 20 $^{\circ}\text{C}$ (pH 7.0). Lowering the pH to 6.2 resulted in an average K_{Pi} value of 17 mM at 10 $^{\circ}\text{C}$, weakening to 28 mM at 40 $^{\circ}\text{C}$. Thus a differential response of slow myosin to Pi was observed with temperature, with the slow myosin while starting off less sensitive to Pi at 10 $^{\circ}\text{C}$ becoming more sensitive to Pi at 40 $^{\circ}\text{C}$.

ADP affinity in the presence of phosphate ($K_{\text{ADP+Pi}}$) was evaluated as for the ADP affinity but using fixed amounts of inorganic phosphate (30 mM in the case of ^{Pso}S1 and 15 mM with ^{Mass}S1). The presence of 30 mM Pi weakened the ADP affinity ($K_{\text{ADP+Pi}}$) for actin.^{Pso}S1 3-4-fold (from about 170 μM to 890 μM at 20 $^{\circ}\text{C}$ (pH 7.0)) as shown in Figure 5A and Table 1. Repeating the measurement at different

temperatures showed the apparent K_{ADP} weakening from around 500 μM at 10-20 $^{\circ}\text{C}$ to 942 μM at 30 $^{\circ}\text{C}$ (Fig 5C and Table 1). For *masseter* the effects of Pi were less marked, with the K_{ADP} weakening only 1-2-fold across the temperature range at pH 7.0. Overall, it appears that phosphate competes with ADP binding to fast A.M, but has little effect on ADP binding in slow A.M.

Lowering the pH to 6.2 resulted in a smaller effect of phosphate on the ADP affinity for actin. $^{P50}\text{S1}$, changing only 2-fold from 228 to 514 μM at 20 $^{\circ}\text{C}$ (compared to the 3 to 4-fold change seen at pH 7.0). This reduced effect of phosphate was seen across the temperature range used. In actin. $^{Mass}\text{S1}$, 15 mM Pi weakened the ADP affinity 2-fold from 47 to 94 μM at 20 $^{\circ}\text{C}$, and a similar 2-fold weakening of the K_{ADP} in phosphate (K_{ADP+Pi}) was seen at the other temperatures used at pH 6.2.

Apparent phosphate affinity ($K_{Pi\ app}$)

The apparent affinity of phosphate for acto-myosinS1 ($K_{Pi\ app}$) in the presence of ADP was calculated from the ADP affinities measured in the absence (K_{ADP}) and presence of phosphate (K_{ADP+Pi}) as detailed in the methods. At pH 7.0 and low temperature the $K_{Pi\ app}$ of actin. $^{P50}\text{S1}$ was similar to the K_{Pi} value measured (11mM and 16 mM, respectively at 10 $^{\circ}\text{C}$). At higher temperatures the K_{Pi} of actin. $^{P50}\text{S1}$ was weakened to 30-40 mM, the $K_{Pi\ app}$ however remained at about 10 mM for the whole temperature range used.

At pH 6.2 the K_{Pi} of *psoas* was 30 % tighter than at pH 7.0 but otherwise showed the same behavior as temperature was increased (weakening from 15 mM at 10 $^{\circ}\text{C}$ to 32 mM at 40 $^{\circ}\text{C}$). The $K_{Pi\ app}$ however appears 2-fold weaker at pH 6.2 for *psoas* with 24 mM and tightens to about 16 mM as temperature is increased.

For actin. $^{Mass}\text{S1}$ we observed a different behavior of the apparent phosphate affinity; while the measured K_{Pi} values at pH 7.0 were similar to *psoas* across the temperature range used, the $K_{Pi\ app}$ showed distinct temperature dependence, weakening from 10 to 40 mM with temperature. The K_{Pi} values of *masseter* were unaffected by a change in pH to 6.2 and remained similar to *psoas* at 22 and 35 mM (10 and 20 $^{\circ}\text{C}$, respectively). The $K_{Pi\ app}$ however lost its temperature dependence

when the pH was lowered to 6.2 and the value remained relatively unaffected at 10-15 mM for actin.^{Mass}S1 throughout the temperature range used.

Relevance to working muscle. Work by us and others indicated an important role for Pi in tension generation as conditions that affect actomyosin affinity affect, in proportion, force generation. With the assumption that A.M force-generating states are in an effective equilibrium with the non-force-generating states at the beginning of the working stroke, past skinned psoas fiber work suggested that, with increasing [Pi] the free energy of the states that precede Pi release decrease as $-RT \ln[\text{Pi}]$ (from the slope of the force- $\ln[\text{Pi}]$ relationship, relative to the free energy of states after Pi release, leading to progressive depopulation of the force-generating states and thus reducing tension generation (26). Earlier observations by Tesi et al (44) highlighted differences between slow and fast myofibrils in tension response to phosphate, with indications of stronger actomyosin bonds in slow muscle. The combination of low pH and high Pi was shown to synergistically inhibit velocity of contraction in skinned fibres (29, 34) adding further support to the notion that in fatigue conditions, the combined effect of Pi and protons on muscle performance would come about either by decreasing the force per bridge and/or increasing the number of low-force bridges. These and other studies indicated that the effect of Pi on its own is moderate at higher temperatures but in combination with low pH it can substantially affect muscle power by affecting actomyosin interaction. The present work adds important information to explain how Pi's interaction changes the ADP affinity for AM and ultimately ATP-induced dissociation of AM, thus the speed of the cross-bridge cycle.

Concluding remarks

The phenomena we studied are at a lower level of component configuration, solution actin and myosin S1. We cannot there account for myosin cooperativity and coordinated responses to load, which could affect the hypothesized limiting processes. While experimental data imply such cooperativities (1) emerging behaviors are difficult to assess and model, a situation further complicated by the difficulty of incorporating intra-head actions into models (31). It remains to be seen

how our findings can be intergraded at the higher level ‘behavior’ of large myosin ensembles interacting with actin filaments, outside or inside an organized sarcomere. It is expected that in such situations other laws may apply when the myosin type effect on contractile behavior is further modulated depending on interactions with intracellular factors and overall muscle action regulation.

We expect that, given the undisputed phenotypic effect of myosin types as observed in mammalian physiology, our data provide highly relevant insights in the mechanochemical coupling factors that distinguish the fiber types. Phosphate dependence of ATP-induced dissociation is modulated by variations in actin affinity. Such variations could help modulate the phosphate dependence of force and velocity, and may explain why phosphate sensitivity appears to be in part temperature-and muscle type-dependent.

Acknowledgements

The authors acknowledge support from various sources as follows:

MAG was supported by the British Heart Foundation grant PG30200. Also, CK, MAG research was co-financed by the European Union (European Social Fund – ESF) and Greek national funds through the Operational Program “Educational and Lifelong Learning” of the National Strategic Reference Framework (NSRF) – Research Funding Program: Thales (MuscleFun Project-MIS 377260) Investing in knowledge society through the European Social Fund.

CK thanks COST Action CM1306 ‘Understanding Movement and Mechanism in Molecular Machines’ for relevant networking support.

References

1. **Baker JE.** Muscle force emerges from dynamic actin-myosin networks, not from independent force generators. *American journal of physiology Cell physiology* 284: C1678; author reply C1678-1679, 2003.
2. **Bloemink MJ, Adamek N, Reggiani C, and Geeves MA.** Kinetic analysis of the slow skeletal myosin MHC-1 isoform from bovine masseter muscle. *Journal of molecular biology* 373: 1184-1197, 2007.
3. **Bloemink MJ, and Geeves MA.** Shaking the myosin family tree: biochemical kinetics defines four types of myosin motor. *Seminars in cell & developmental biology* 22: 961-967, 2011.
4. **Bogdanis GC.** Effects of physical activity and inactivity on muscle fatigue. *Frontiers in physiology* 3: 142, 2012.
5. **Bogdanis GC, Nevill ME, Lakomy HK, and Boobis LH.** Power output and muscle metabolism during and following recovery from 10 and 20 s of maximal sprint exercise in humans. *Acta physiologica Scandinavica* 163: 261-272, 1998.
6. **Bottinelli R.** Functional heterogeneity of mammalian single muscle fibres: do myosin isoforms tell the whole story? *Pflugers Archiv : European journal of physiology* 443: 6-17, 2001.
7. **Cannon DT, Howe FA, Whipp BJ, Ward SA, McIntyre DJ, Ladroue C, Griffiths JR, Kemp GJ, and Rossiter HB.** Muscle metabolism and activation heterogeneity by combined 31P chemical shift and T2 imaging, and pulmonary O2 uptake during incremental knee-extensor exercise. *Journal of applied physiology* 115: 839-849, 2013.
8. **Cooke R.** Force generation in muscle. *Current opinion in cell biology* 2: 62-66, 1990.
9. **Cooke R.** Modulation of the actomyosin interaction during fatigue of skeletal muscle. *Muscle & nerve* 36: 756-777, 2007.
10. **Cooke R, Franks K, Luciani GB, and Pate E.** The inhibition of rabbit skeletal muscle contraction by hydrogen ions and phosphate. *The Journal of physiology* 395: 77-97, 1988.
11. **Coupland ME, Puchert E, and Ranatunga KW.** Temperature dependence of active tension in mammalian (rabbit psoas) muscle fibres: effect of inorganic phosphate. *The Journal of physiology* 536: 879-891, 2001.
12. **Criddle AH, Geeves MA, and Jeffries T.** The use of actin labelled with N-(1-pyrenyl)iodoacetamide to study the interaction of actin with myosin subfragments and troponin/tropomyosin. *The Biochemical journal* 232: 343-349, 1985.
13. **Crow MT, and Kushmerick MJ.** Correlated reduction of velocity of shortening and the rate of energy utilization in mouse fast-twitch muscle during a continuous tetanus. *The Journal of general physiology* 82: 703-720, 1983.
14. **Debold EP, Beck SE, and Warshaw DM.** Effect of low pH on single skeletal muscle myosin mechanics and kinetics. *American journal of physiology Cell physiology* 295: C173-179, 2008.
15. **Debold EP, Dave H, and Fitts RH.** Fiber type and temperature dependence of inorganic phosphate: implications for fatigue. *American journal of physiology Cell physiology* 287: C673-681, 2004.
16. **Debold EP, Walcott S, Woodward M, and Turner MA.** Direct observation of phosphate inhibiting the force-generating capacity of a miniensemble of Myosin molecules. *Biophysical journal* 105: 2374-2384, 2013.

17. **Egan P, Moore J, Schunn C, Cagan J, and LeDuc P.** Emergent Systems Energy Laws for Predicting Myosin Ensemble Processivity. *PLoS Computational Biology* 11: 2015.
18. **Fitts RH.** Cellular mechanisms of muscle fatigue. *Physiol Rev* 74: 49-94, 1994.
19. **Foley JM, Harkema SJ, and Meyer RA.** Decreased ATP cost of isometric contractions in ATP-depleted rat fast-twitch muscle. *The American journal of physiology* 261: C872-881, 1991.
20. **Geeves MA.** Review: The ATPase mechanism of myosin and actomyosin. *Biopolymers* 105: 483-491, 2016.
21. **Green HJ.** Mechanisms of muscle fatigue in intense exercise. *Journal of sports sciences* 15: 247-256, 1997.
22. **Hamada T, Sale DG, MacDougall JD, and Tarnopolsky MA.** Interaction of fibre type, potentiation and fatigue in human knee extensor muscles. *Acta physiologica Scandinavica* 178: 165-173, 2003.
23. **Huxley HE, and Hanson J.** The structural basis of the contraction mechanism in striated muscle. *Annals of the New York Academy of Sciences* 81: 403-408, 1959.
24. **Iorga B, Adamek N, and Geeves MA.** The slow skeletal muscle isoform of myosin shows kinetic features common to smooth and non-muscle myosins. *The Journal of biological chemistry* 282: 3559-3570, 2007.
25. **Johansen KL, Doyle J, Sakkas GK, and Kent-Braun JA.** Neural and metabolic mechanisms of excessive muscle fatigue in maintenance hemodialysis patients. *American journal of physiology Regulatory, integrative and comparative physiology* 289: R805-813, 2005.
26. **Karatzafiri C, Chinn MK, and Cooke R.** The force exerted by a muscle cross-bridge depends directly on the strength of the actomyosin bond. *Biophysical journal* 87: 2532-2544, 2004.
27. **Karatzafiri C, de Haan A, Ferguson RA, van Mechelen W, and Sargeant AJ.** Phosphocreatine and ATP content in human single muscle fibres before and after maximum dynamic exercise. *Pflugers Archiv : European journal of physiology* 442: 467-474, 2001.
28. **Karatzafiri C, de Haan A, van Mechelen W, and Sargeant AJ.** Metabolic changes in single human fibres during brief maximal exercise. *Experimental physiology* 86: 411-415, 2001.
29. **Karatzafiri C, Franks-Skiba K, and Cooke R.** Inhibition of shortening velocity of skinned skeletal muscle fibers in conditions that mimic fatigue. *Am J Physiol Regul Integr Comp Physiol* 294: R948-955, 2008.
30. **Karatzafiri C, Myburgh KH, Chinn MK, Franks-Skiba K, and Cooke R.** Effect of an ADP analog on isometric force and ATPase activity of active muscle fibers. *American journal of physiology Cell physiology* 284: C816-825, 2003.
31. **Månsson A.** Actomyosin-ADP States, Interhead Cooperativity, and the Force-Velocity Relation of Skeletal Muscle. *Biophysical journal* 98: 1237-1246, 2010.
32. **Margossian SS, and Lowey S.** Interaction of myosin subfragments with F-actin. *Biochemistry* 17: 5431-5439, 1978.
33. **Millar NC, and Geeves MA.** The limiting rate of the ATP-mediated dissociation of actin from rabbit skeletal muscle myosin subfragment 1. *FEBS letters* 160: 141-148, 1983.
34. **Nelson CR, Debold EP, and Fitts RH.** Phosphate and acidosis act synergistically to depress peak power in rat muscle fibers. *American journal of physiology Cell physiology* 307: C939-950, 2014.
35. **Nyitrai M, Rossi R, Adamek N, Pellegrino MA, Bottinelli R, and Geeves MA.** What limits the velocity of fast-skeletal muscle contraction in mammals? *Journal of molecular biology* 355: 432-442, 2006.

36. **Pate E, Bhimani M, Franks-Skiba K, and Cooke R.** Reduced effect of pH on skinned rabbit psoas muscle mechanics at high temperatures: implications for fatigue. *The Journal of physiology* 486 (Pt 3): 689-694, 1995.
37. **Pate E, and Cooke R.** Addition of phosphate to active muscle fibers probes actomyosin states within the powerstroke. *Pflugers Archiv : European journal of physiology* 414: 73-81, 1989.
38. **Reconditi M, Linari M, Lucii L, Stewart A, Sun YB, Narayanan T, Irving T, Piazzesi G, Irving M, and Lombardi V.** Structure-function relation of the myosin motor in striated muscle. *Annals of the New York Academy of Sciences* 1047: 232-247, 2005.
39. **Schiaffino S, and Reggiani C.** Fiber types in mammalian skeletal muscles. *Physiological reviews* 91: 1447-1531, 2011.
40. **Sieck GC, Fournier M, Prakash YS, and Blanco CE.** Myosin phenotype and SDH enzyme variability among motor unit fibers. *Journal of applied physiology* 80: 2179-2189, 1996.
41. **Siemankowski RF, Wiseman MO, and White HD.** ADP dissociation from actomyosin subfragment 1 is sufficiently slow to limit the unloaded shortening velocity in vertebrate muscle. *Proceedings of the National Academy of Sciences of the United States of America* 82: 658-662, 1985.
42. **Spudich JA, and Watt S.** The regulation of rabbit skeletal muscle contraction. I. Biochemical studies of the interaction of the tropomyosin-troponin complex with actin and the proteolytic fragments of myosin. *The Journal of biological chemistry* 246: 4866-4871, 1971.
43. **Tesi C, Colomo F, Nencini S, Piroddi N, and Poggesi C.** The effect of inorganic phosphate on force generation in single myofibrils from rabbit skeletal muscle. *Biophysical journal* 78: 3081-3092, 2000.
44. **Tesi C, Colomo F, Piroddi N, and Poggesi C.** Characterization of the cross-bridge force-generating step using inorganic phosphate and BDM in myofibrils from rabbit skeletal muscles. *The Journal of physiology* 541: 187-199, 2002.
45. **Walklate J, and Geeves MA.** Temperature manifold for a stopped-flow machine to allow measurements from -10 to +40 degrees C. *Analytical biochemistry* 476: 11-16, 2015.
46. **Weeds AG, and Taylor RS.** Separation of subfragment-1 isoenzymes from rabbit skeletal muscle myosin. *Nature* 257: 54-56, 1975.
47. **Westerblad H, Allen DG, and Lannergren J.** Muscle fatigue: lactic acid or inorganic phosphate the major cause? *News in physiological sciences : an international journal of physiology produced jointly by the International Union of Physiological Sciences and the American Physiological Society* 17: 17-21, 2002.
48. **Westerblad H, Bruton JD, and Lannergren J.** The effect of intracellular pH on contractile function of intact, single fibres of mouse muscle declines with increasing temperature. *The Journal of physiology* 500 (Pt 1): 193-204, 1997.

Figures & Captions

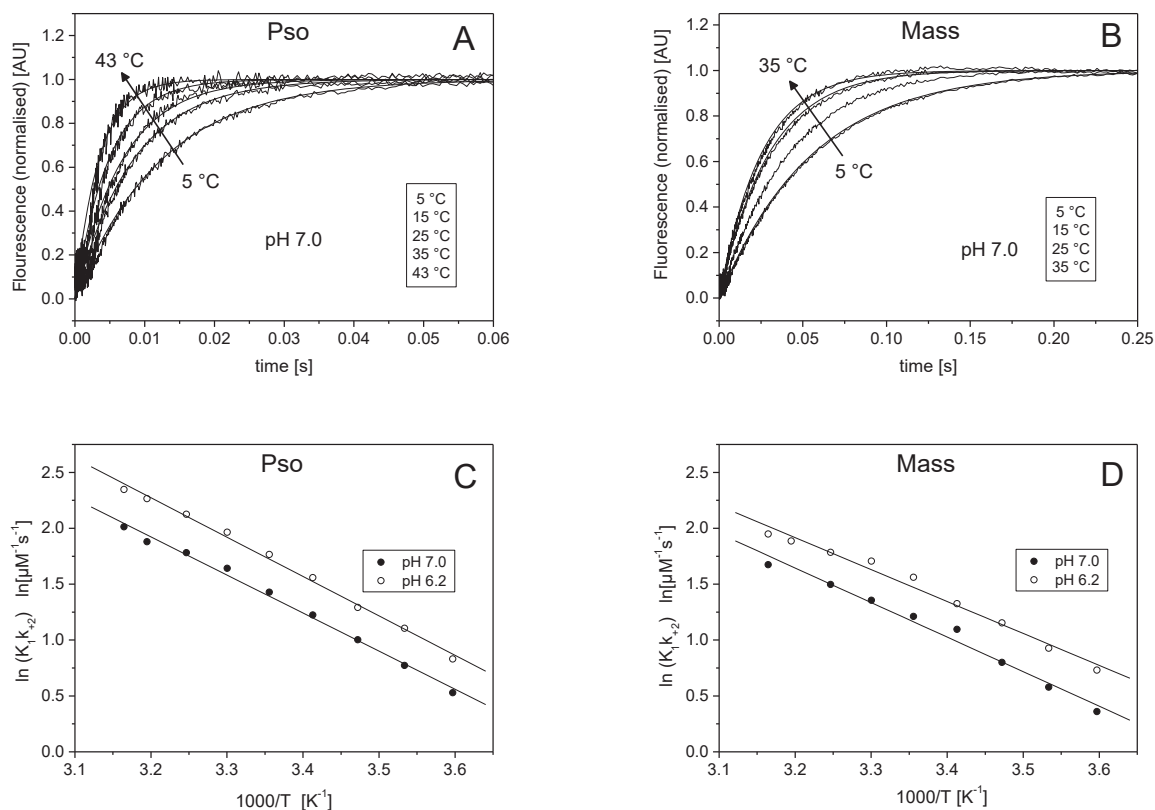


Figure 1. ATP-induced dissociation of S1 from actin, for fast (Pso) and slow (Mass) myosin isoform, at pH 7.0 and 6.2, in a range of temperatures. A. Normalized transients observed when mixing 0.5 μM pyr-act.PsoS1 with 25 μM ATP in pH 7.0 buffer at different temperatures (selected transients are shown). The change in fluorescence was fitted to a single exponential equation (best fits superimposed), giving k_{obs} of 84.8, 136.2, 208.5, 296.9, and 374.4 s^{-1} for 5, 15, 25, 35 and 43 $^{\circ}\text{C}$, respectively. The amplitudes of the transients were relatively stable at 46 % of total fluorescence change, with some loss observed at temperatures above 30 $^{\circ}\text{C}$. B. Normalized transients observed when mixing 0.5 μM pyrAct.MassS1 with 25 μM ATP in pH 7.0 buffer at different temperatures (selected transients are shown). The change in fluorescence was fitted to a single exponential equation (best fits superimposed), giving observed rate constants of 26.7, 36.1, 46.7, and 64.9 s^{-1} for 5, 15, 25 and 35 $^{\circ}\text{C}$, respectively. The amplitudes of the transients were relatively stable at 40 % of total fluorescence change, with some loss observed at temperatures above 30 $^{\circ}\text{C}$. C. Arrhenius plot of the $k_{\text{obs}}/[\text{ATP}] = K_1 k_{+2}$ of Pso at pH 7.0 and pH 6.2 (temperature range 5 – 43 $^{\circ}\text{C}$). The linear fits (best fits superimposed) gave slopes of -3.41 ± 0.10 and -3.52 ± 0.09 K for pH 7.0 and 6.2, respectively, from which the activation energies (E_a) were calculated as 28.3 ± 0.8 and 29.3 ± 0.8 kJ/mol. D. Arrhenius plot of the $k_{\text{obs}}/[\text{ATP}] = K_1 k_{+2}$ of Mass at pH 7.0 and pH 6.2 (temperature range 5 – 43 $^{\circ}\text{C}$). The linear fits (best fits superimposed) gave slopes of -3.09 ± 0.17 and -2.86 ± 0.14 K for pH 7.0 and 6.2, respectively, from which the activation energies (E_a) were calculated as 25.7 ± 1.4 and 23.8 ± 1.1 kJ/mol.

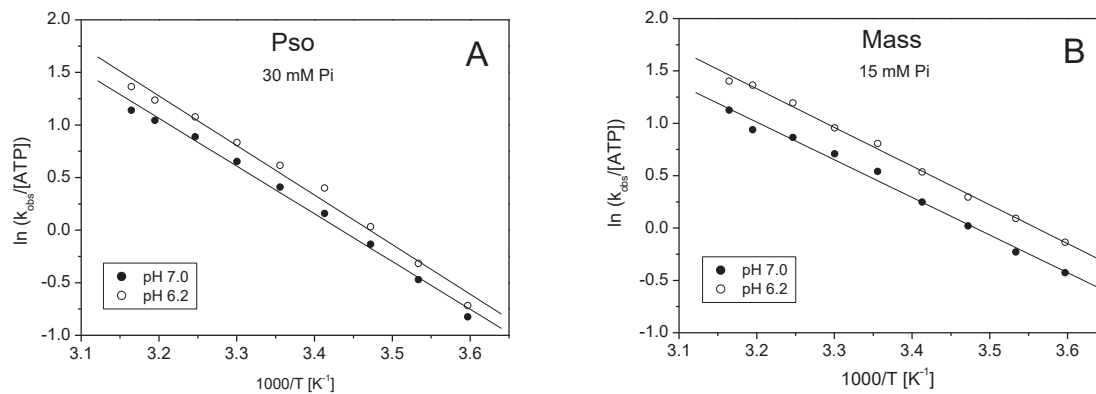


Figure 2. Effect of inorganic phosphate on the ATP-induced dissociation of S1 from actin, for fast (Pso) and slow (Mass) myosin isoform at pH 7.0 and 6.2, in a range of temperatures. A. Arrhenius plot of the k_{obs} of *Psoas* at pH 7.0 and pH 6.2 in the presence of 30 mM Pi. The linear fits (best fits superimposed) gave slopes of -4.54 ± 0.15 and -4.71 ± 0.20 K for pH 7.0 and 6.2, respectively, from which the activation energies (E_a) were calculated as 37.7 ± 1.2 and 39.2 ± 1.6 kJ/mol. B. Arrhenius plot of the k_{obs} of *Masseter* at pH 7.0 and pH 6.2 in the presence of 15 mM Pi. The linear fits (best fits superimposed) gave slopes of -3.59 ± 0.13 and -3.694 ± 0.08 K for pH 7.0 and 6.2, respectively, from which the activation energies (E_a) were calculated as 29.9 ± 1.1 and 30.7 ± 0.7 kJ/mol.

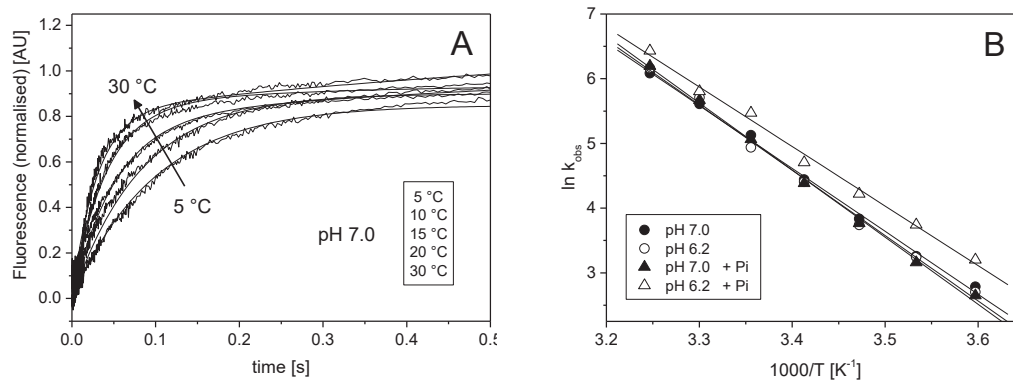


Figure 3. Temperature dependence of the ADP release from pyrAct.MassS1.A. Normalized fluorescent transients observed when 0.5 μM pyrAct.MassS1 pre-incubated with 75 μM ADP was mixed with 8 mM ATP at different temperatures between 5 and 30 $^{\circ}\text{C}$ in pH 7.0 buffer (selected transients are shown). The change in fluorescence was biphasic when observed over a time scale of 5 sec, however here only the initial fast phase is shown (fits superimposed). The k_{obs} for the fast phase were 16.2, 26.0, 46.3, 85.0 and 273 s^{-1} for 5, 10, 15, 20 and 30 $^{\circ}\text{C}$, respectively. B. Arrhenius plot of the k_{obs} of the ADP release rate constant of *Masseter* at pH 7.0 and pH 6.2 in the absence and presence of 15 mM Pi. The linear fits (best fits superimposed) gave slopes of -9.72 ± 0.24 and -10.09 ± 0.33 K for pH 7.0 and 6.2, and -10.36 ± 0.23 and -9.20 ± 0.31 K for pH 7.0+Pi and pH 6.2 +Pi, respectively. The activation energies (E_a) were calculated as 75.9 ± 4.1 and 84.7 ± 6.1 kJ/mol for pH 7.0 and 6.2 without phosphate, and 94.4 ± 5.0 and 88.9 ± 3.9 kJ/mol for pH 7.0 and pH 6.2 respectively in the presences of phosphate.

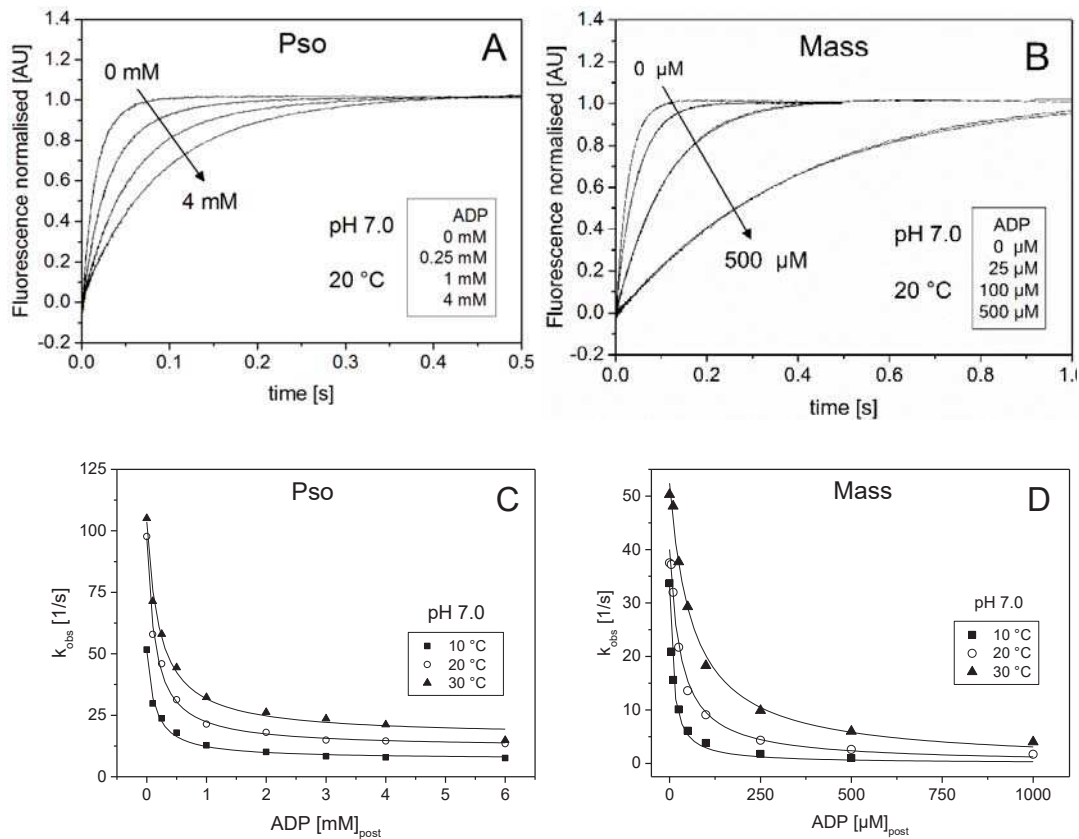


Figure 4. Temperature dependence of the ADP affinity (K_{AD}) for fast (*Pso*) and slow (*Mass*) A.S1 at pH 7.0. A. Normalized fluorescent transients observed when 0.5 μ M pyrAct.*Pso*S1 was mixed with 25 μ M ATP with various concentrations of ADP present at 20 °C in pH 7.0 buffer. The change in fluorescence was fitted by a single exponential equation (best fits superimposed). The k_{obs} determined were 87.7, 45.9, 21.4 and 14.5 s^{-1} for zero, 0.25, 1 and 4 mM ADP, respectively, with an amplitude of 30 % of total fluorescence. B. Fluorescent transients observed when 0.5 μ M pyrAct.*Mass*S1 was mixed with 25 μ M ATP with various concentrations of ADP present at 20 °C in pH 7.0 buffer. The change in fluorescence was fitted to a single exponential equation (best fits superimposed). The k_{obs} determined were 37.5, 21.7, 9.1 and 2.6 s^{-1} for zero, 25, 100 and 500 μ M ADP, respectively, with an amplitude of 30 % of total fluorescence. C. Plot of the observed rate constants as a function of [ADP]_{post} for *Psoas* in pH 7.0 buffer at 10, 20 and 30 °C. The data sets were fitted to a hyperbole to obtain the ADP affinity (K_{AD}) for each temperature: $131 \pm 16 \mu$ M (10 °C), $140 \pm 14 \mu$ M (20 °C) and $213 \pm 29 \mu$ M (30 °C) for the depicted data. Refer to Table 1 for average values for from measurements in different days. D. Plot of the observed rate constants as a function of [ADP]_{post} for *Masseter* in pH 7.0 buffer at 10, 20 and 30 °C. The data sets were fitted to a hyperbole to obtain the ADP affinity (K_{AD}) for each temperature: $9.6 \pm 0.7 \mu$ M (10 °C), $31.3 \pm 4.0 \mu$ M (20 °C) and $62.4 \pm 6.1 \mu$ M (30 °C) for the depicted data. Refer to Table 1 for average values from measurements in different days.

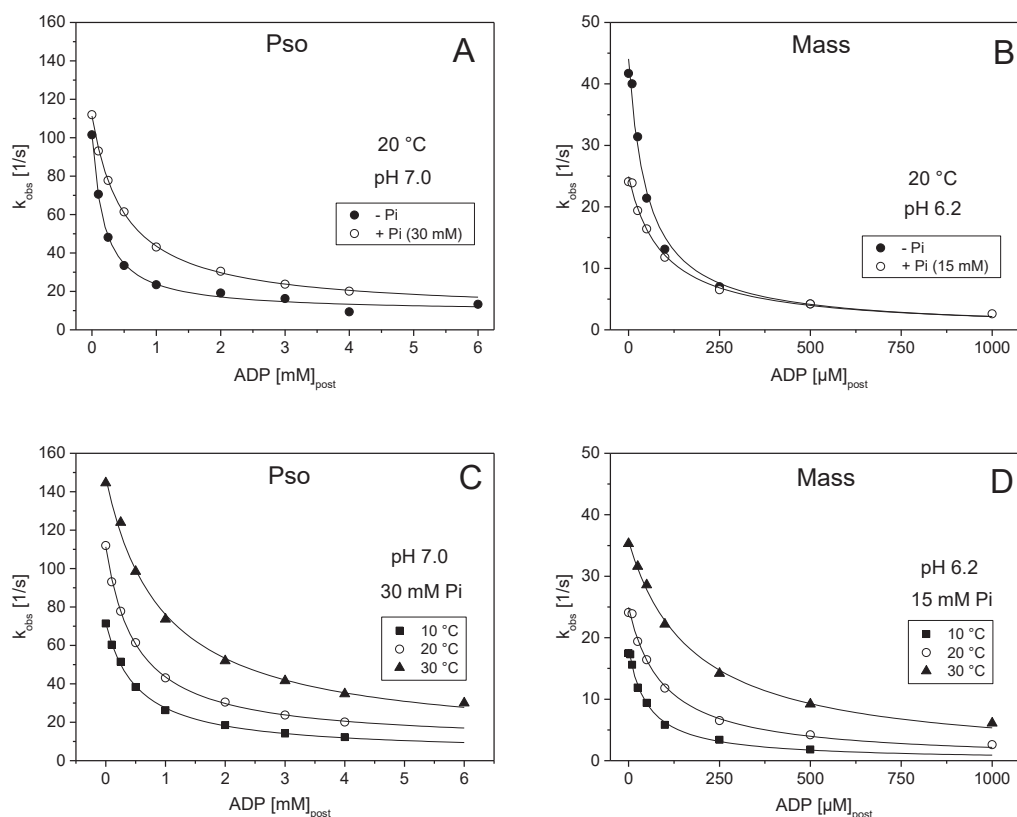


Figure 5. Effect of phosphate (Pi) on the K_{AD} of fast (*Pso*) and slow (*Mass*) A.S1. A. Plot of the observed rate constants as a function of [ADP] for *Psoas* in the presence and absence of added 30 mM Pi (pH 7.0 buffer at 20 °C). The data sets were fitted to a hyperbole to obtain the ADP affinity (K_{AD}) \pm Pi: $175 \pm 22 \mu\text{M}$ (no Pi) and $510 \pm 22 \mu\text{M}$ (with Pi). Refer to Table 1 for average values for from measurements in different days. B. Plot of the observed rate constants as a function of [ADP] for *Masseter* in the presence and absence of added 15 mM Pi (pH 6.2 buffer at 20 °C). The data sets were fitted to a hyperbole to obtain the ADP affinity (K_{AD}) \pm Pi: $48.4 \pm 6.8 \mu\text{M}$ (no Pi) and $94.5 \pm 8.1 \mu\text{M}$ (with Pi). Refer to Table 1 for average values for from measurements in different days. C. Plot of the observed rate constants as a function of [ADP] for *Psoas* in pH 7.0 buffer in the presence of added 30 mM Pi at 10, 20 and 30 °C. The data sets were fitted to a hyperbole to obtain the ADP affinity (K_{AD}) for each temperature: $530 \pm 36 \mu\text{M}$ (10 °C), $510 \pm 22 \mu\text{M}$ (20 °C) and $942 \pm 117 \mu\text{M}$ (30 °C). Refer to Table 1 for average values for from measurements in different days. D. Plot of the observed rate constants as a function of [ADP] for *Masseter* in pH 6.2 buffer in the presence of added 15 mM Pi at 10, 20 and 30 °C. The data sets were fitted to a hyperbole to obtain the ADP affinity (K_{AD}) for each temperature: $52.2 \pm 5.8 \mu\text{M}$ (10 °C), $94.5 \pm 8.1 \mu\text{M}$ (20 °C) and $175.3 \pm 9.7 \mu\text{M}$ (30 °C). Refer to Table 1 for average values for from measurements in different days.

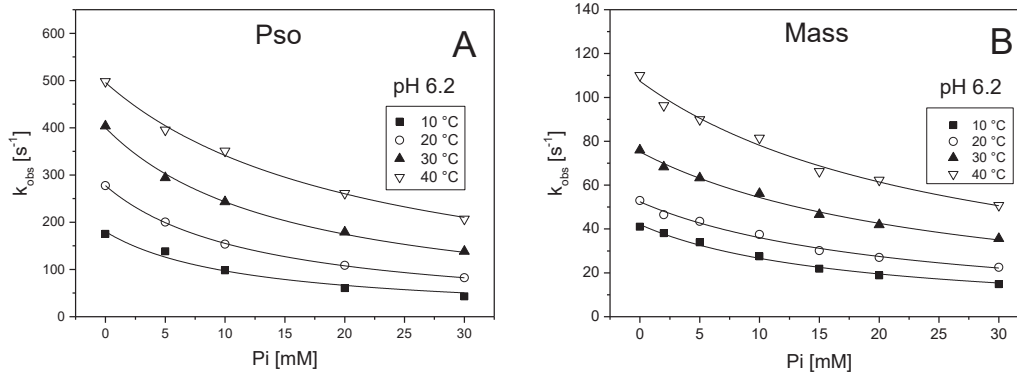


Figure 6. Phosphate (Pi) affinity for A.M in the absence of ADP (phosphate) at pH 6.2, for fast (Pso) and slow (Mass) myosin isoform. A. Plot of the observed rate constants of the ATP-induced dissociation of $0.5 \mu M$ pyrAct.S1 by $50 \mu M$ ATP as a function of $[Pi]$ for *Psoas* (pH 6.2 buffer) at 10 to 40 °C. The data sets were fitted to a hyperbole to obtain the Pi affinity (K_{pi}) for each temperature: 11.7 ± 1.8 mM (10 °C), 12.7 ± 0.2 mM (20 °C), 15.5 ± 0.7 mM (30 °C) and 22.1 ± 1.2 mM (40 °C). Refer to Table 1 for average values for from measurements in different days. B. Plot of the observed rate constants of the ATP-induced dissociation of $0.5 \mu M$ pyrAct.S1 by $25 \mu M$ ATP as a function of $[Pi]$ for *Masseter* (pH 6.2 buffer) at 10 to 40 °C. The data sets were fitted to a hyperbole to obtain the Pi affinity (K_{pi}) for each temperature: 17.3 ± 1.1 mM (10 °C), 22.0 ± 1.4 mM (20 °C), 26.1 ± 1.3 mM (30 °C) and 26.7 ± 2.1 mM (40 °C). Refer to Table 1 for average values for from measurements in different days.

Tables

Table 1. Average values of kinetic parameters describing the ATP induced dissociation rate of actin.S1 for psoas and masseter myosin, in pH 7 and 6.2, under different temperatures, in the absence or presence of added phosphate.

pH	Psoas S1								Masseter S1							
	7.0				6.2				7.0				6.2			
	<i>constant</i>	K_{AD}	$K_{AD} + Pi^*$	K_{PI}	<i>calc. K_{PI}</i>	K_{AD}	$K_{AD} + Pi^*$	K_{PI}	<i>calc. K_{PI}</i>	K_{AD}	$K_{AD} + Pi^{**}$	K_{PI}	<i>calc. K_{PI}</i>	K_{AD}	$K_{AD} + Pi^{**}$	K_{PI}
<i>units</i>	μM	μM	mM	mM	μM	μM	mM	mM	μM	μM	mM	mM	μM	μM	mM	mM
10 °C	201 ±34 (n=2)	770 ±37 (n=3)	16.2 ± 1.1 (n=2)	10.6	256 ±32 (n=2)	665 ±39 (n=2)	11.5 ±1.1 (n=3)	18.8	10.3 ±1.2 (n=2)	22.5 ±2.9 (n=2)	22.3 ±4.1 (n=1)	10.8	21.8 ±1.3 (n=3)	52.2 ± 4.2 (n=2)	16.6 ±0.6 (n=3)	10.8
20 °C	203 ±13 (n=4)	919 ±72 (n=3)	28.3 ±1.8 (n=2)	8.5	228 ±36 (n=2)	463 ±52 (n=1)	15.6 ±1.7 (n=4)	23.9	29.7 ±2.8 (n=2)	44.4 ±4.6 (n=2)	35.0 ±4.4 (n=1)	30.9	46.8 ±3.4 (n=3)	82.6 ±5.7 (n=2)	21.3 ±0.9 (n=3)	14.7
30 °C	232 ± 29 (n=2)	1017 ±52 (n=3)	31.1 ±3.0 (n=2)	8.9	236 ±29 (n=2)	926 ±73 (n=2)	20.5 ±2.0 (n=4)	10.3	56.2 ±6.5 (n=2)	79.3 ±6.5 (n=2)		40.3	83.9 ±4.7 (n=3)	174.6 ±7.0 (n=2)	25.3 ±1.0 (n=3)	14.2
40 °C			41.1 ±7.8 (n=2)				31.1 ±1.6 (n=4)								27.9 ±1.7 (n=2)	

*30 mM Pi

**15 mM Pi

Table 2. Thermodynamics results (E_A values) describing the temperature dependence of the dissociation rate constant for psoas (Pso) and masseter (Mass) myosin, under pH 7 and 6.2.

		Pso		Mass	
constant	\pm Pi	pH 7.0	pH 6.2	pH 7.0	pH 6.2
K_1k_{+2} [kJ/mol]	-	28.3 ± 0.8	29.3 ± 0.8	25.7 ± 1.4	23.8 ± 1.1
K_1k_{+2} [kJ/mol]	+	37.7 ± 1.2	39.2 ± 1.6	29.9 ± 1.1	30.7 ± 0.7
k_{-AD} [kJ/mol]	-	N/A	N/A	75.9 ± 4.1	84.7 ± 6.1
k_{-AD} [kJ/mol]	+	N/A	N/A	94.4 ± 5.0	88.9 ± 3.9

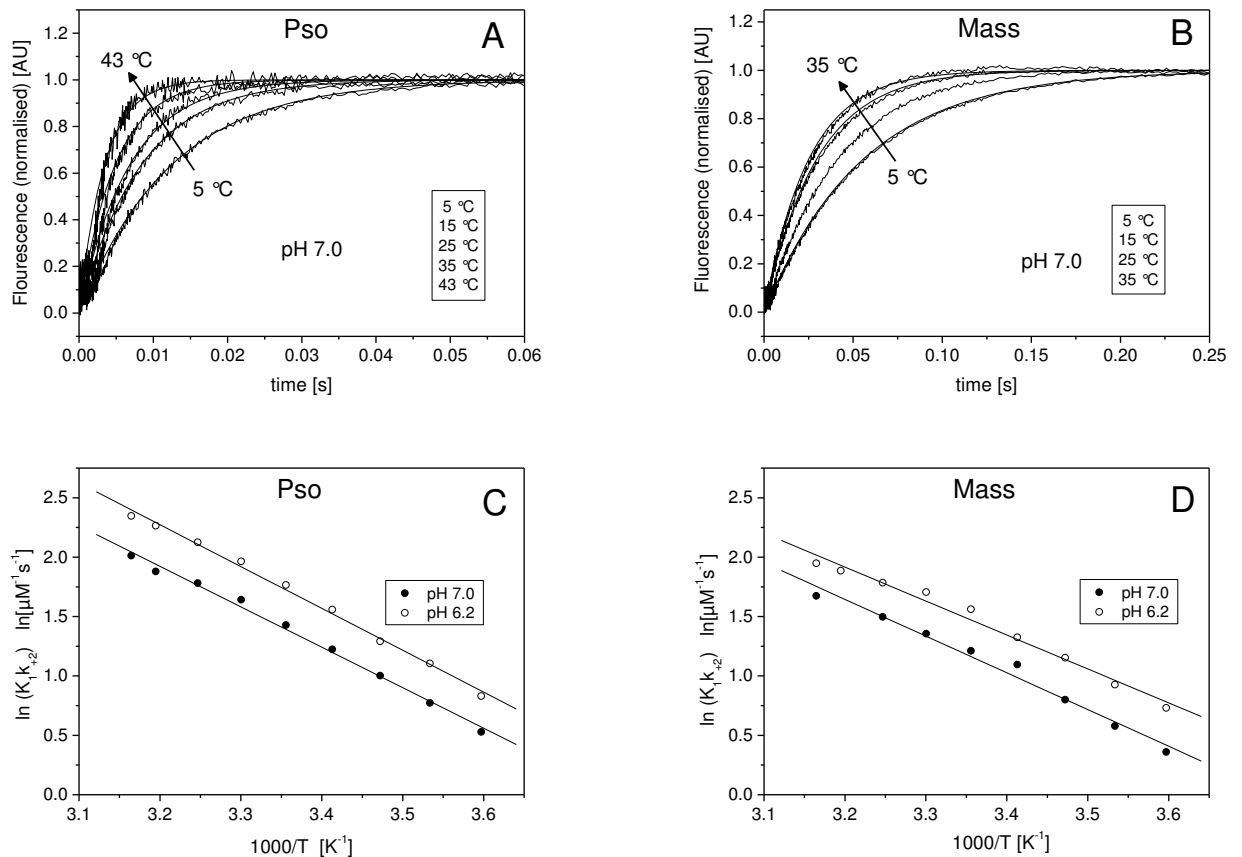


Figure 1. ATP-induced dissociation of S1 from actin, for fast (Pso) and slow (Mass) myosin isoform, at pH 7.0 and 6.2, in a range of temperatures. A. Normalized transients observed when mixing 0.5 μM pyr-act.PsoS1 with 25 μM ATP in pH 7.0 buffer at different temperatures (selected transients are shown). The change in fluorescence was fitted to a single exponential equation (best fits superimposed), giving k_{obs} of 84.8, 136.2, 208.5, 296.9, and 374.4 s^{-1} for 5, 15, 25, 35 and 43 $^{\circ}\text{C}$, respectively. The amplitudes of the transients were relatively stable at 46 % of total fluorescence change, with some loss observed at temperatures above 30 $^{\circ}\text{C}$. B. Normalized transients observed when mixing 0.5 μM pyrAct.MassS1 with 25 μM ATP in pH 7.0 buffer at different temperatures (selected transients are shown). The change in fluorescence was fitted to a single exponential equation (best fits superimposed), giving observed rate constants of 26.7, 36.1, 46.7, and 64.9 s^{-1} for 5, 15, 25 and 35 $^{\circ}\text{C}$, respectively. The amplitudes of the transients were relatively stable at 40 % of total fluorescence change, with some loss observed at temperatures above 30 $^{\circ}\text{C}$. C. Arrhenius plot of the $k_{\text{obs}}/[\text{ATP}] = K_1k_{+2}$ of Pso at pH 7.0 and pH 6.2 (temperature range 5 – 43 $^{\circ}\text{C}$). The linear fits (best fits superimposed) gave slopes of -3.41 ± 0.10 and -3.52 ± 0.09 K for pH 7.0 and 6.2, respectively, from which the activation energies (E_a) were calculated as 28.3 ± 0.8 and 29.3 ± 0.8 kJ/mol. D. Arrhenius plot of the $k_{\text{obs}}/[\text{ATP}] = K_1k_{+2}$ of Mass at pH 7.0 and pH 6.2 (temperature range 5 – 43 $^{\circ}\text{C}$). The linear fits (best fits superimposed) gave slopes of -3.09 ± 0.17 and -2.86 ± 0.14 K for pH 7.0 and 6.2, respectively, from which the activation energies (E_a) were calculated as 25.7 ± 1.4 and 23.8 ± 1.1 kJ/mol.

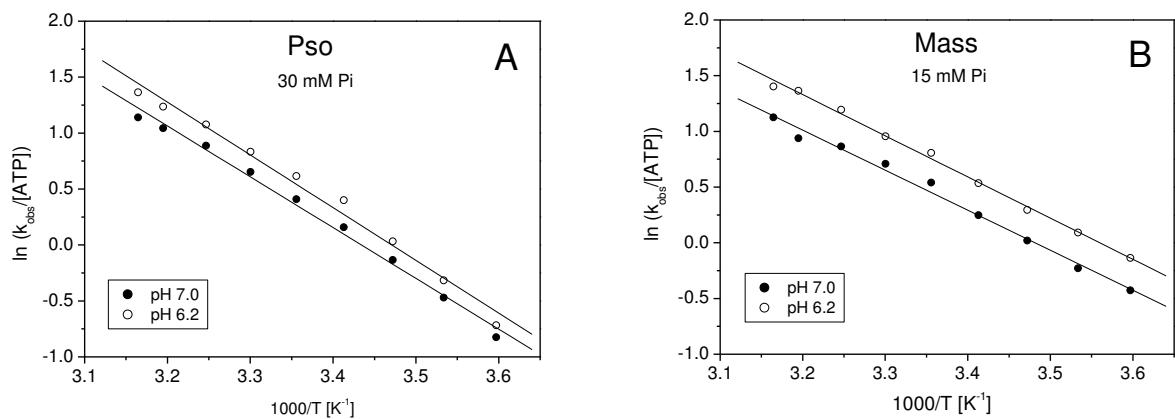


Figure 2. Effect of inorganic phosphate on the ATP-induced dissociation of S1 from actin, for fast (Pso) and slow (Mass) myosin isoform at pH 7.0 and 6.2, in a range of temperatures. A. Arrhenius plot of the k_{obs} of *Psoas* at pH 7.0 and pH 6.2 in the presence of 30 mM Pi. The linear fits (best fits superimposed) gave slopes of -4.54 ± 0.15 and -4.71 ± 0.20 K for pH 7.0 and 6.2, respectively, from which the activation energies (E_a) were calculated as 37.7 ± 1.2 and 39.2 ± 1.6 kJ/mol. B. Arrhenius plot of the k_{obs} of *Masseter* at pH 7.0 and pH 6.2 in the presence of 15 mM Pi. The linear fits (best fits superimposed) gave slopes of -3.59 ± 0.13 and -3.694 ± 0.08 K for pH 7.0 and 6.2, respectively, from which the activation energies (E_a) were calculated as 29.9 ± 1.1 and 30.7 ± 0.7 kJ/mol.

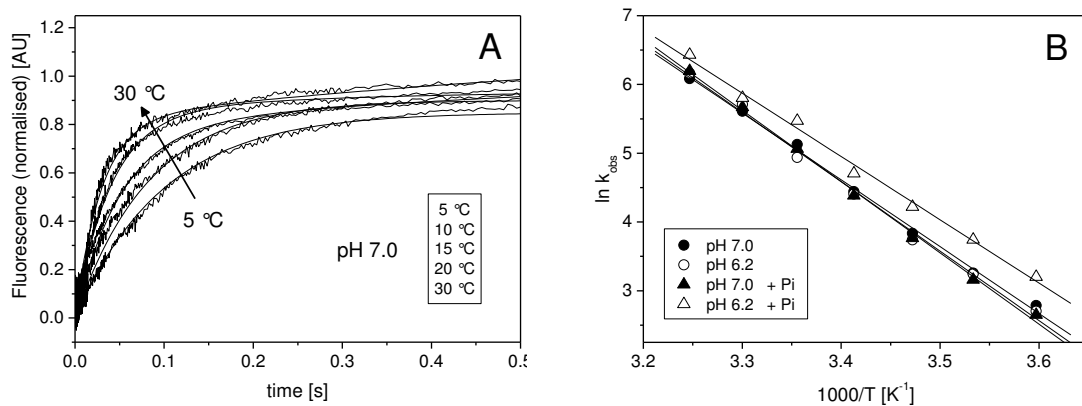


Figure 3. Temperature dependence of the ADP release from pyrAct.MassS1.A. Normalized fluorescent transients observed when 0.5 μM pyrAct.MassS1 pre-incubated with 75 μM ADP was mixed with 8 mM ATP at different temperatures between 5 and 30 $^{\circ}\text{C}$ in pH 7.0 buffer (selected transients are shown). The change in fluorescence was biphasic when observed over a time scale of 5 sec, however here only the initial fast phase is shown (fits superimposed). The k_{obs} for the fast phase were 16.2, 26.0, 46.3, 85.0 and 273 s^{-1} for 5, 10, 15, 20 and 30 $^{\circ}\text{C}$, respectively. B. Arrhenius plot of the k_{obs} of the ADP release rate constant of *Masseter* at pH 7.0 and pH 6.2 in the absence and presence of 15 mM Pi. The linear fits (best fits superimposed) gave slopes of -9.72 ± 0.24 and -10.09 ± 0.33 K for pH 7.0 and 6.2, and -10.36 ± 0.23 and -9.20 ± 0.31 K for pH 7.0+Pi and pH 6.2 +Pi, respectively. The activation energies (E_a) were calculated as 75.9 ± 4.1 and 84.7 ± 6.1 kJ/mol for pH 7.0 and 6.2 without phosphate, and 94.4 ± 5.0 and 88.9 ± 3.9 kJ/mol for pH 7.0 and pH 6.2 respectively in the presences of phosphate.

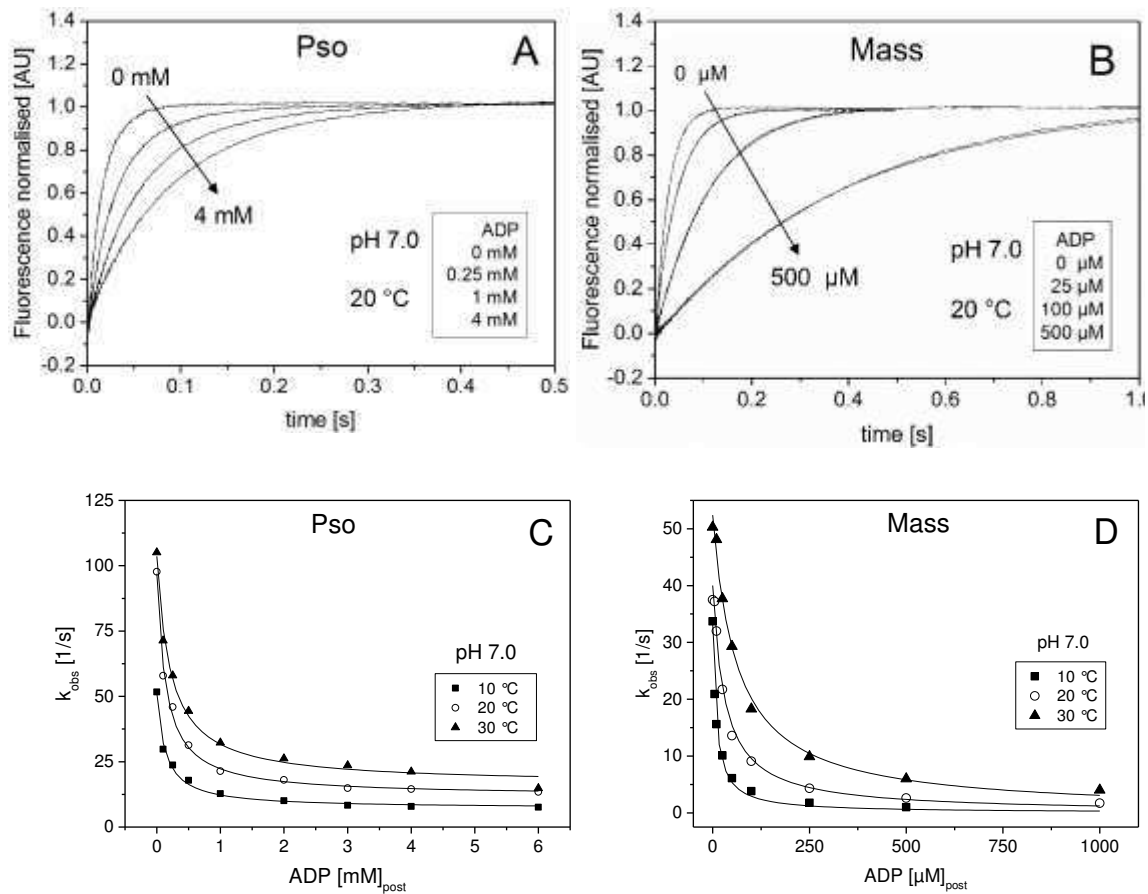


Figure 4. Temperature dependence of the ADP dissociation constant (K_{ADP}) for fast (*Pso*) and slow (*Mass*) A.S1 at pH 7.0. A. Normalized fluorescent transients observed when 0.5 μM *pyrAct.PsoS1* was mixed with 25 μM ATP with various concentrations of ADP present at 20 $^{\circ}\text{C}$ in pH 7.0 buffer. The change in fluorescence was fitted by a single exponential equation (best fits superimposed). The k_{obs} determined were 87.7, 45.9, 21.4 and 14.5 s^{-1} for zero, 0.25, 1 and 4 mM ADP, respectively, with an amplitude of 30 % of total fluorescence. B. Fluorescent transients observed when 0.5 μM *pyrAct.MassS1* was mixed with 25 μM ATP with various concentrations of ADP present at 20 $^{\circ}\text{C}$ in pH 7.0 buffer. The change in fluorescence was fitted to a single exponential equation (best fits superimposed). The k_{obs} determined were 37.5, 21.7, 9.1 and 2.6 s^{-1} for zero, 25, 100 and 500 μM ADP, respectively, with an amplitude of 30 % of total fluorescence. C. Plot of the observed rate constants as a function of [ADP] for *Psoas* in pH 7.0 buffer at 10, 20 and 30 $^{\circ}\text{C}$. The data sets were fitted to a hyperbole to obtain the ADP dissociation constant (K_{ADP}) for each temperature: 131 ± 16 μM (10 $^{\circ}\text{C}$), 140 ± 14 μM (20 $^{\circ}\text{C}$) and 213 ± 29 μM (30 $^{\circ}\text{C}$) for the depicted data. Refer to Table 1 for average values for from measurements in different days. D. Plot of the observed rate constants as a function of [ADP] for *Masseter* in pH 7.0 buffer at 10, 20 and 30 $^{\circ}\text{C}$. The data sets were fitted to a hyperbole to obtain the ADP dissociation constant (K_{ADP}) for each temperature: 9.6 ± 0.7 μM (10 $^{\circ}\text{C}$), 31.3 ± 4.0 μM (20 $^{\circ}\text{C}$) and 62.4 ± 6.1 μM (30 $^{\circ}\text{C}$) for the depicted data. Refer to Table 1 for average values from measurements in different days.

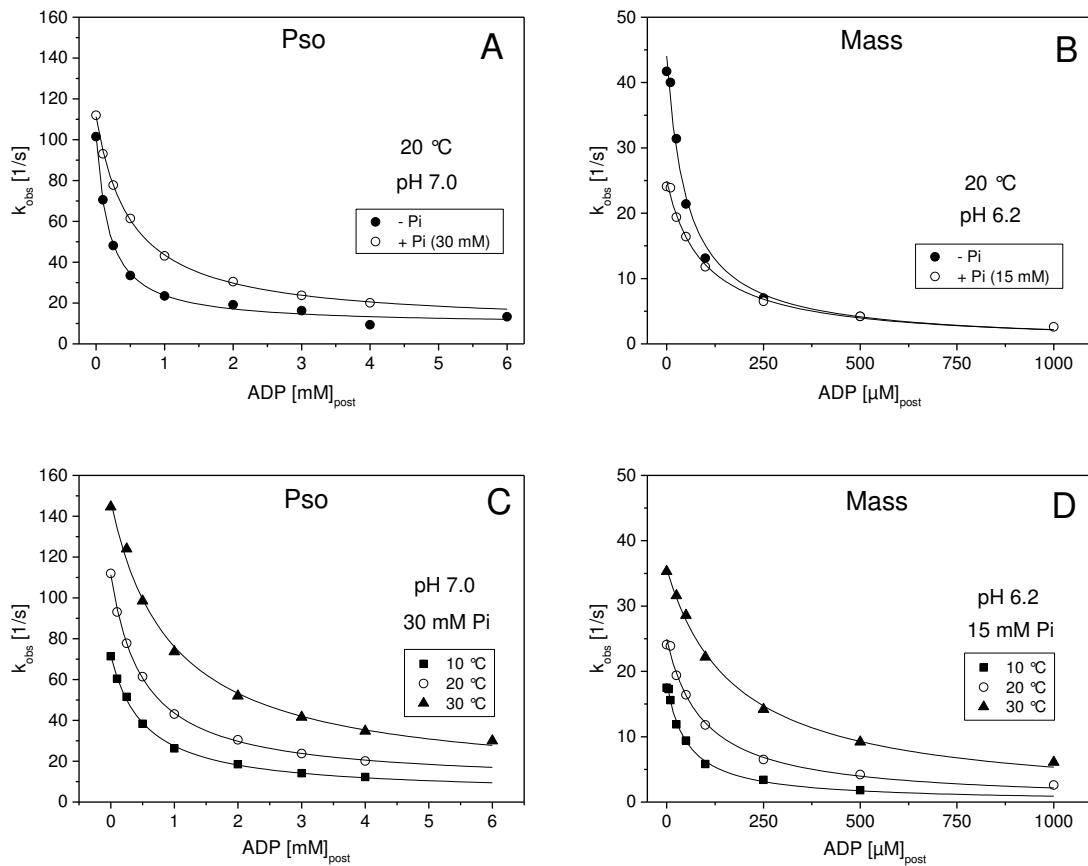


Figure 5. Effect of phosphate (Pi) on the K_{AD} of fast (*Pso*) and slow (*Mass*) A.S1. A. Plot of the observed rate constants as a function of [ADP] for *Psoas* in the presence and absence of added 30 mM Pi (pH 7.0 buffer at 20 °C). The data sets were fitted to a hyperbole to obtain the ADP dissociation constant (K_{ADP}) \pm Pi: $175 \pm 22 \mu\text{M}$ (no Pi) and $510 \pm 22 \mu\text{M}$ (with Pi). Refer to Table 1 for average values for from measurements in different days. B. Plot of the observed rate constants as a function of [ADP] for *Masseter* in the presence and absence of added 15 mM Pi (pH 6.2 buffer at 20 °C). The data sets were fitted to a hyperbole to obtain the ADP dissociation constant (K_{ADP}) \pm Pi: $48.4 \pm 6.8 \mu\text{M}$ (no Pi) and $94.5 \pm 8.1 \mu\text{M}$ (with Pi). Refer to Table 1 for average values for from measurements in different days. C. Plot of the observed rate constants as a function of [ADP] for *Psoas* in pH 7.0 buffer in the presence of added 30 mM Pi at 10, 20 and 30 °C. The data sets were fitted to a hyperbole to obtain the ADP dissociation constant (K_{ADP}) for each temperature: $530 \pm 36 \mu\text{M}$ (10 °C), $510 \pm 22 \mu\text{M}$ (20 °C) and $942 \pm 117 \mu\text{M}$ (30 °C). Refer to Table 1 for average values for from measurements in different days. D. Plot of the observed rate constants as a function of [ADP] for *Masseter* in pH 6.2 buffer in the presence of added 15 mM Pi at 10, 20 and 30 °C. The data sets were fitted to a hyperbole to obtain the ADP dissociation constant (K_{ADP}) for each temperature: $52.2 \pm 5.8 \mu\text{M}$ (10 °C), $94.5 \pm 8.1 \mu\text{M}$ (20 °C) and $175.3 \pm 9.7 \mu\text{M}$ (30 °C). Refer to Table 1 for average values for from measurements in different days.

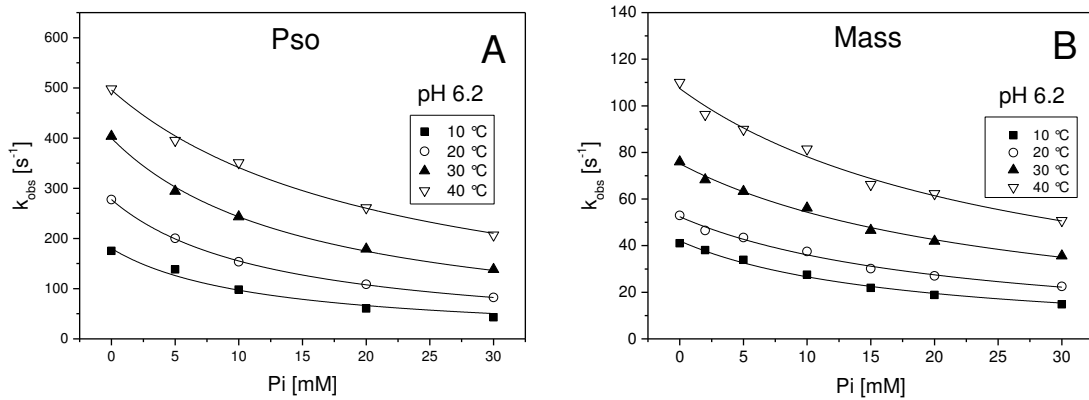


Figure 6. Phosphate (Pi) dissociation constant for A.M in the absence of ADP (phosphate) at pH 6.2, for fast (Pso) and slow (Mass) myosin isoform. A. Plot of the observed rate constants of the ATP-induced dissociation of 0.5 μM pyrAct.S1 by 50 μM ATP as a function of [Pi] for *Psoas* (pH 6.2 buffer) at 10 to 40 $^{\circ}\text{C}$. The data sets were fitted to a hyperbole to obtain the Pi dissociation constant (K_{pi}) for each temperature: 11.7 ± 1.8 mM (10 $^{\circ}\text{C}$), 12.7 ± 0.2 mM (20 $^{\circ}\text{C}$), 15.5 ± 0.7 mM (30 $^{\circ}\text{C}$) and 22.1 ± 1.2 mM (40 $^{\circ}\text{C}$). Refer to Table 1 for average values for from measurements in different days. B. Plot of the observed rate constants of the ATP-induced dissociation of 0.5 μM pyrAct.S1 by 25 μM ATP as a function of [Pi] for *Masseter* (pH 6.2 buffer) at 10 to 40 $^{\circ}\text{C}$. The data sets were fitted to a hyperbole to obtain the Pi dissociation constant (K_{pi}) for each temperature: 17.3 ± 1.1 mM (10 $^{\circ}\text{C}$), 22.0 ± 1.4 mM (20 $^{\circ}\text{C}$), 26.1 ± 1.3 mM (30 $^{\circ}\text{C}$) and 26.7 ± 2.1 mM (40 $^{\circ}\text{C}$). Refer to Table 1 for average values for from measurements in different days.

Tables

Table 1. Average values of kinetic parameters describing the ATP induced dissociation rate of actin.S1 for psoas and masseter myosin, in pH 7 and 6.2, under different temperatures, in the absence or presence of added phosphate.

pH	Psoas S1								Masseter S1							
	7.0				6.2				7.0				6.2			
constant	K_{ADP}	K_{ADP+PI}^*	K_{PI}	calc. K_{PI}	K_{ADP}	K_{ADP+PI}^*	K_{PI}	calc. K_{PI}	K_{ADP}	K_{ADP+PI}^{**}	K_{PI}	calc. K_{PI}	K_{ADP}	K_{ADP+PI}^{**}	K_{PI}	calc. K_{PI}
units	μ M	μ M	mM	mM	μ M	μ M	mM	mM	μ M	μ M	mM	mM	μ M	μ M	mM	mM
10 °C	201 ±34 (n=2)	770 ±37 (n=3)	16.2 ± 1.1 (n=2)	10.6	256 ±32 (n=2)	665 ±39 (n=2)	11.5 ±1.1 (n=3)	18.8	10.3 ±1.2 (n=2)	22.5 ±2.9 (n=2)	22.3 ±4.1 (n=1)	10.8	21.8 ±1.3 (n=3)	52.2 ± 4.2 (n=2)	16.6 ±0.6 (n=3)	10.8
20 °C	203 ±13 (n=4)	919 ±72 (n=3)	28.3 ±1.8 (n=2)	8.5	228 ±36 (n=2)	463 ±52 (n=1)	15.6 ±1.7 (n=4)	23.9	29.7 ±2.8 (n=2)	44.4 ±4.6 (n=2)	35.0 ±4.4 (n=1)	30.9	46.8 ±3.4 (n=3)	82.6 ±5.7 (n=2)	21.3 ±0.9 (n=3)	14.7
30 °C	232 ± 29 (n=2)	1017 ±52 (n=3)	31.1 ±3.0 (n=2)	8.9	236 ±29 (n=2)	926 ±73 (n=2)	20.5 ±2.0 (n=4)	10.3	56.2 ±6.5 (n=2)	79.3 ±6.5 (n=2)		40.3	83.9 ±4.7 (n=3)	174.6 ±7.0 (n=2)	25.3 ±1.0 (n=3)	14.2
40 °C			41.1 ±7.8 (n=2)				31.1 ±1.6 (n=4)								27.9 ±1.7 (n=2)	

*30 mM Pi

**15 mM Pi

Table 2. Thermodynamics results (E_A values) describing the temperature dependence of the dissociation rate constant for psoas (Pso) and masseter (Mass) myosin, under pH 7 and 6.2.

		Pso		Mass	
constant	\pm Pi	pH 7.0	pH 6.2	pH 7.0	pH 6.2
K_1k_{+2} [kJ/mol]	-	28.3 ± 0.8	29.3 ± 0.8	25.7 ± 1.4	23.8 ± 1.1
K_1k_{+2} [kJ/mol]	+	37.7 ± 1.2	39.2 ± 1.6	29.9 ± 1.1	30.7 ± 0.7
k_{-AD} [kJ/mol]	-	N/A	N/A	75.9 ± 4.1	84.7 ± 6.1
k_{-AD} [kJ/mol]	+	N/A	N/A	94.4 ± 5.0	88.9 ± 3.9